Lattice QCD Inputs for Neutrino-Nucleon Scattering

Raza Sabbir Sufian

Theory Seminar

BROOKHAVEN NATIONAL LABORATORY

April 3, 2019

Jefferson Lab
Thomas Jefferson National Accelerator Facility

Neutrino Physics

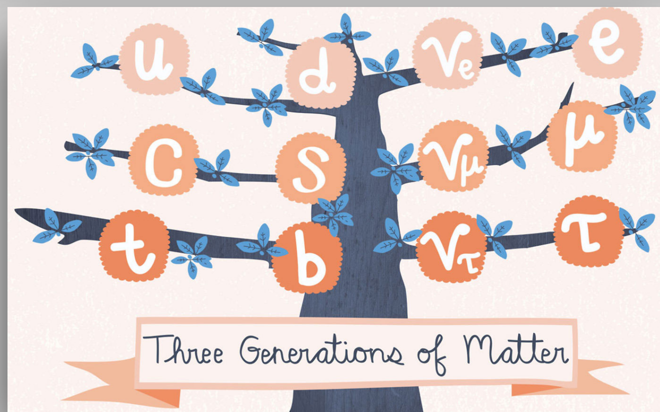

Elementary

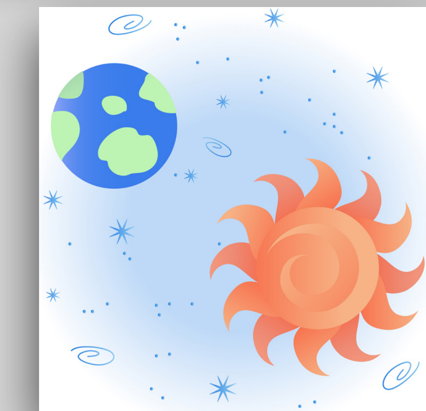

Diverse source

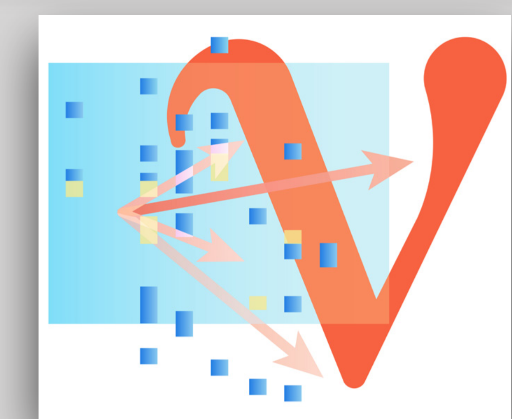

Elusive

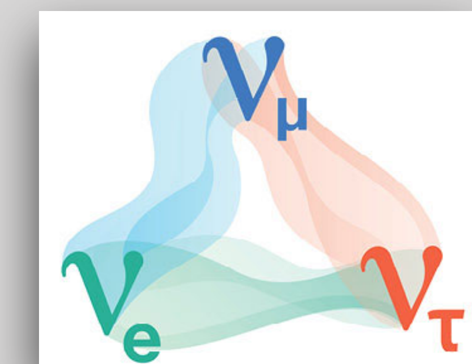

Oscillate

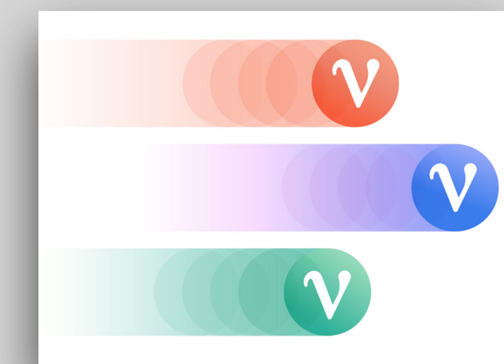

Lightweight (extremely)

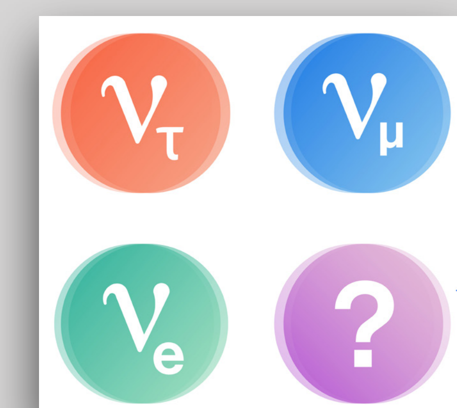

Sterile neutrino?

Their own antiparticles?

neutrinos.fnal.gov

Neutrino Scattering Experiment

Deep Underground
Neutrino Experiment

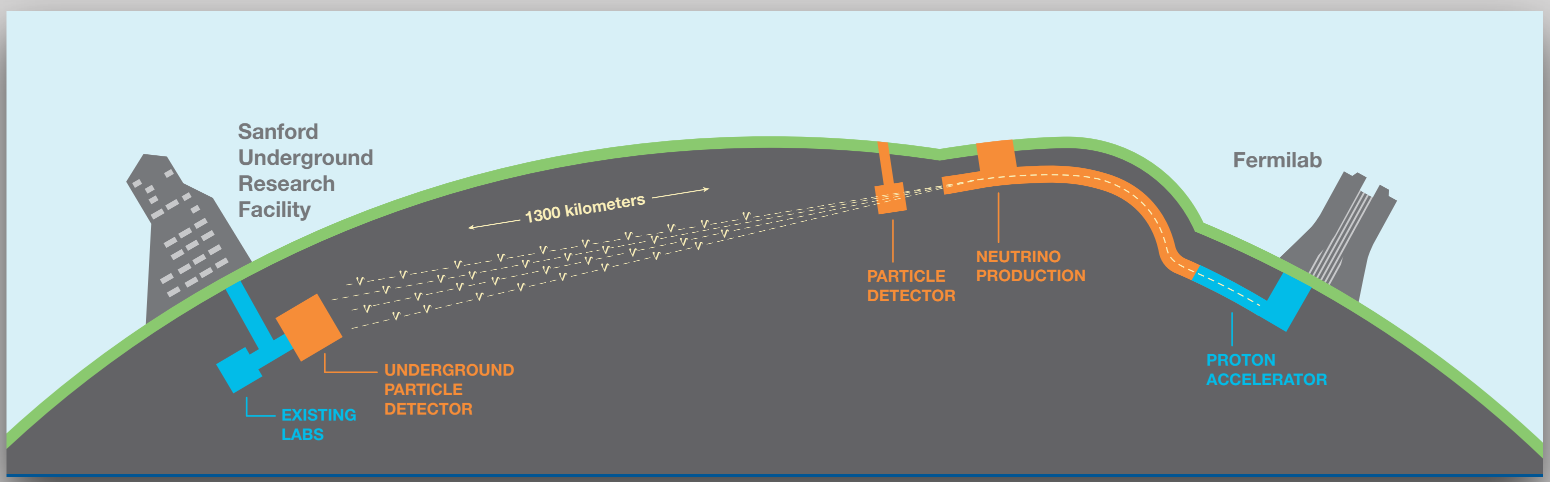

Neutrino scattering experiments on nucleus

What we observe in detector

Neutrino flux

$\otimes$

Neutrino-nucleon cross sections

$\otimes$

Nuclear effects

$\otimes$

Detector properties and effects

★ Neutrino beam energy

E_ν

Incoming neutrino Energy

What experimentalists want

E_{detected}

$$E_\nu = \frac{M_p}{cos\theta_p(1+2M_p/T_p)^{1/2} - 1}$$

$$Q^2 = 2M_pT_p$$

What experimentalists get

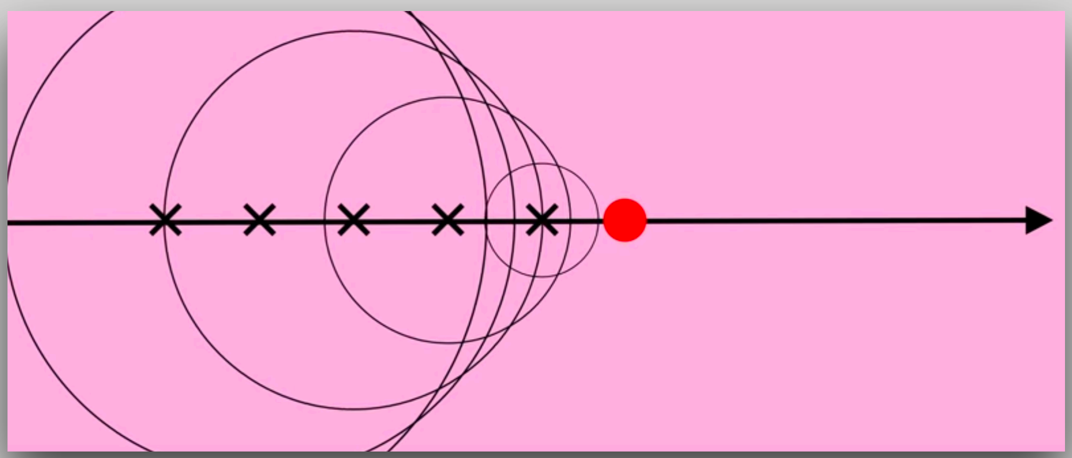

Neutrino oscillation probability is a function of E_ν

$$P_{\nu_\alpha \to \nu_\beta} \propto exp\left(-i\frac{\Delta m^2 t}{2E_\nu}\right)$$

$t \approx L$: Distance between source and detector

Challenges: Neutrino Scattering Experiment

★ Particle configuration and kinematics of interaction within the nucleus are unknown

★ Rely on Monte Carlo event generator to produce probability weighted maps to connect detector observation with true kinematics

★ Initially produced hadronic shower propagates thorough nucleus

★ **Final state interaction**

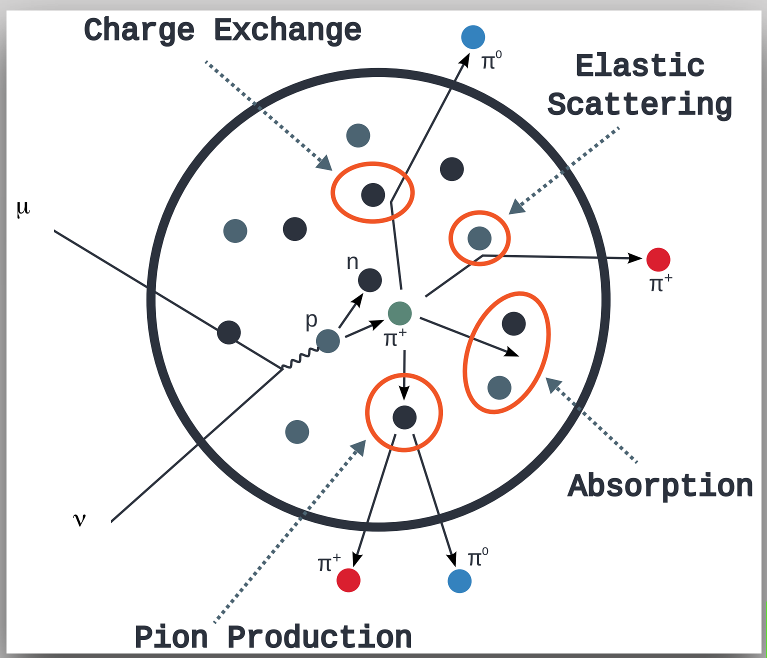

Nucleon-nucleon interactions

Pion-nucleon interactions

NuSTEC white paper

Challenges: Neutrino Scattering Experiment

★ **Absence of widely accepted and universal nuclear models**

Data from MiniBooNE & MINERvA

T2K Analysis , PRD 93, 072010 (2016)

Best-fit parameter values for the fits to all datasets simultaneously.

Fit type	χ^2/N_{DOF}	M_{A} (GeV/c^2)	2p2h norm (%)
RFG + rel RPA + 2p2h	97.8/228	1.15 ± 0.03	27 ± 12
RFG + nonrel RPA + 2p2h	117.9/228	1.07 ± 0.03	34 ± 12
SF + 2p2h	97.5/228	1.33 ± 0.02	0 (at limit)

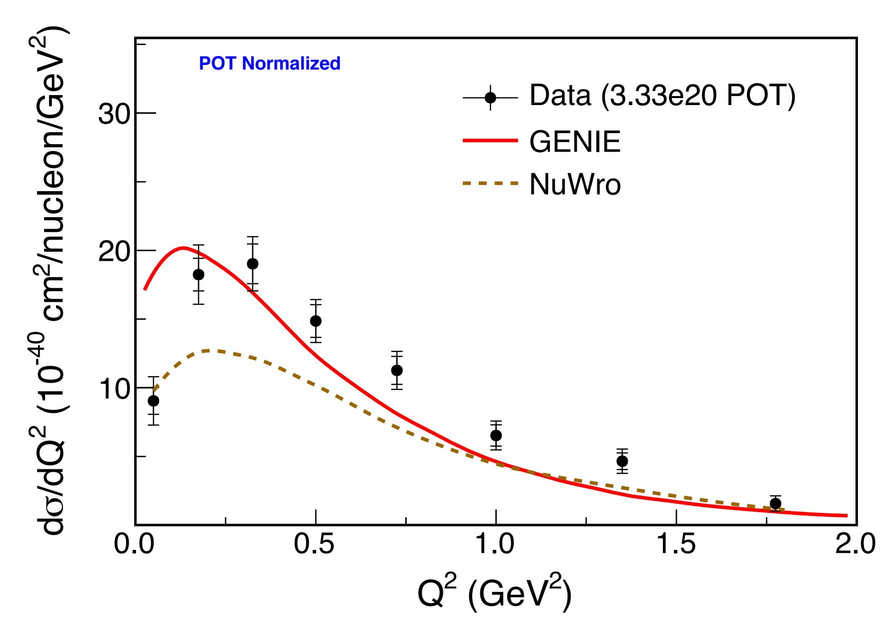

$$\nu_\mu + \mathrm{CH} \to \mu^- \pi^0 + \mathrm{nucleon(s)}$$

PRD 96, 072003 (2017)

★ For neutrino-nucleon CCQE scattering, often mentioned and assumed axial mass M_A (in the dipole formula) as the only unknown parameter

Neutrino Scattering Experiment

From experiment (with many complexities) → **Neutrino-nucleus scattering cross sections**

Isolate nuclear effects using nuclear models

Fundamental interaction at play → **Neutrino interaction with quarks through**
Z-boson (neutral current interaction)
W-boson (charged current interaction)

Nuclear models are still very important

One goal : Lattice QCD calculation of neutrino-nucleon scattering cross section without depending on nuclear models

Lattice QCD Efforts for Neutrino-Nucleon Scattering

★ Lattice QCD calculation of **valence** and **sea** u,d,s quarks contribution to nucleon electromagnetic form factors

★ Phenomenological calculation of (anti)neutrino-nucleon neutral current scattering differential cross sections

★ Lattice calculation of nucleon axial form factor at 170 MeV pion mass

★ Phenomenological constraint on $s(x) - \bar{s}(x)$ distribution

★ First lattice QCD calculation of charm quark electromagnetic form factors

Lattice QCD Efforts

Advertisement : Hadron Structure Using Current-Current Correlations

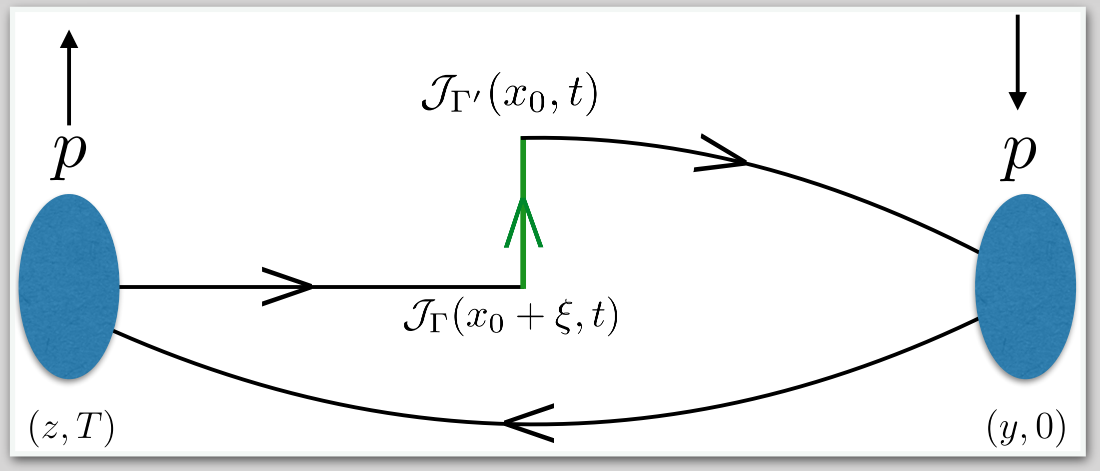

Factorization

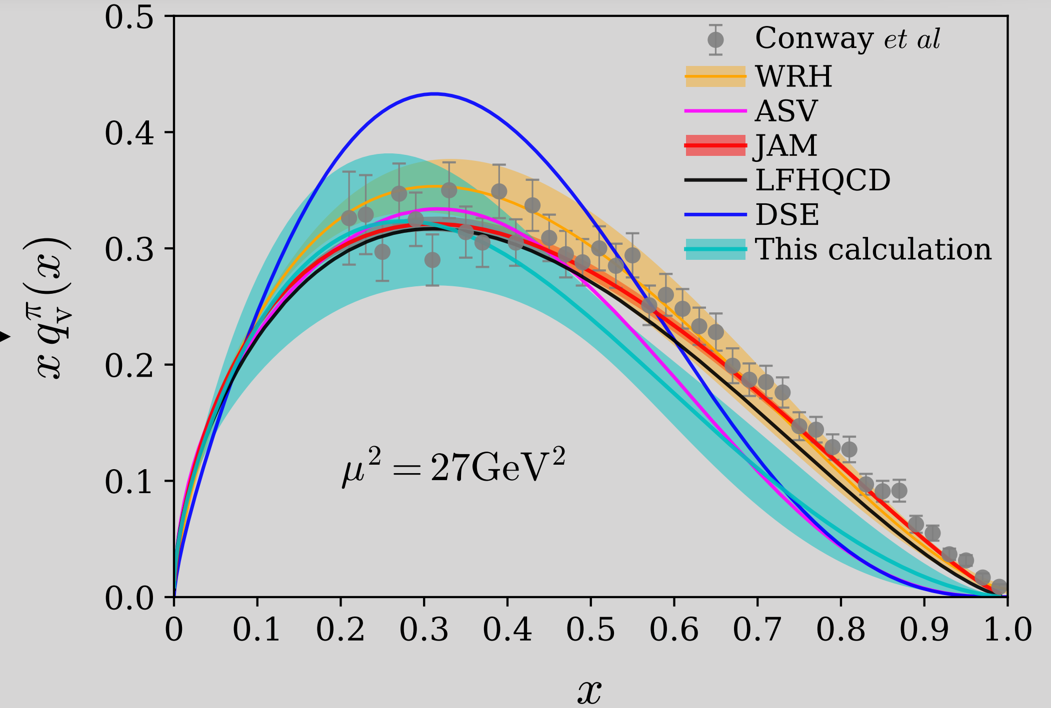

RSS, Karpie, Egerer, Qiu, Richards, Orginos
PRD (in press) 2019

- ★ Many current combinations are possible
- ★ Which one to pick? — clue is in neutrino-nucleon scattering

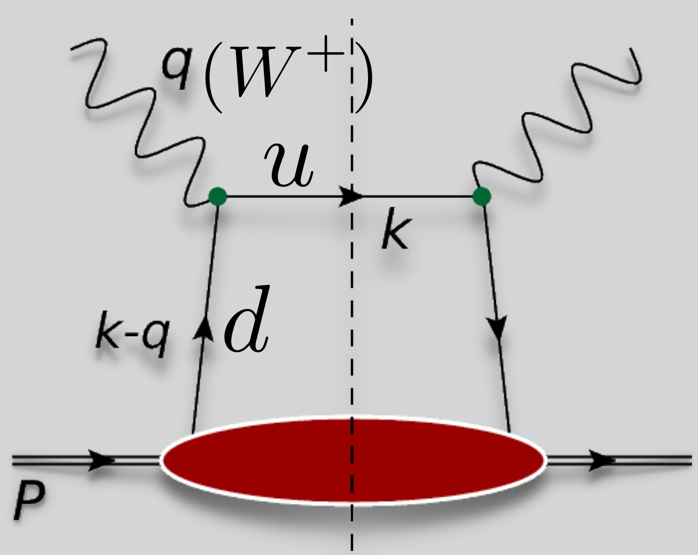

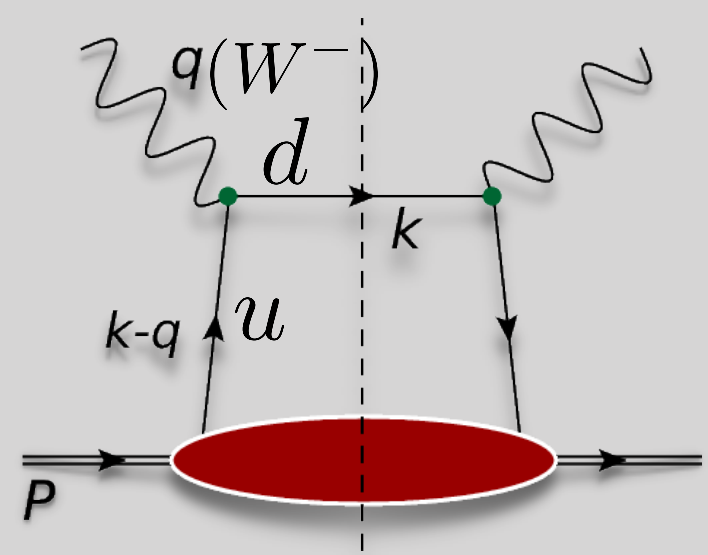

$$W^{\mu\nu} = (-g^{\mu\nu} + q^\mu q^\nu/q^2)F_1(x,Q^2) + \frac{(P^\mu - q^\mu P\cdot q/q^2)(P^\nu - q^\nu P\cdot q/q^2)}{P\cdot q}F_2(x,Q^2) - i\epsilon^{\mu\nu\alpha\beta}\frac{q_\alpha P_\beta}{2P\cdot q}F_3(x,Q^2)$$

$$F_3^{W^+} + F_3^{W^-} = 2[u - \bar{u} + d - \bar{d} + s - \bar{s} + c - \bar{c}]$$

★ We are interested in neutral current scattering

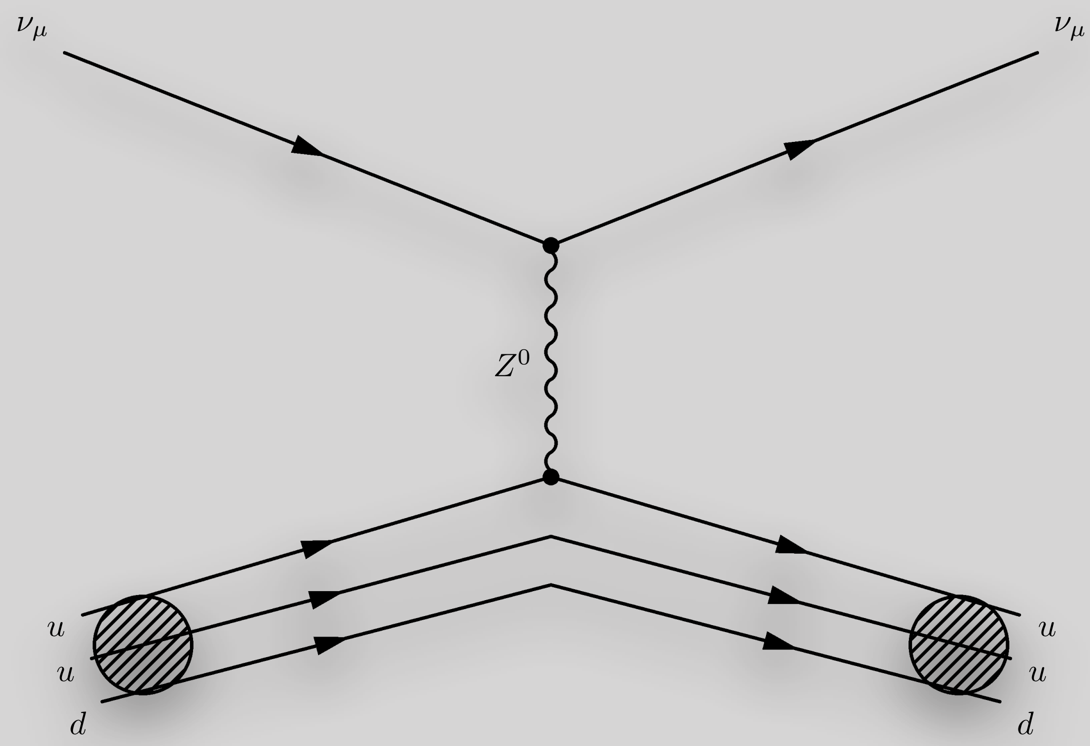

Matrix element in V-A structure of leptonic current

$$M = \frac{i}{2\sqrt{2}} G_F \underbrace{\bar{\nu}(q_2)\gamma_\mu(1-\gamma_5)\nu(q_1)}_{\text{leptonic current}} \underbrace{\langle N(p_2)|J^\mu_Z|N(p_1)\rangle}_{\text{hadronic current}} .$$

$$\boxed{\langle N(p_2)|\, J^\mu_Z\, |N(p_1)\rangle = \bar{u}(p_2)[F_1^Z(Q^2) + F_2^Z(Q^2)\frac{i\sigma^{\mu\nu}q_\nu}{2M_N} + F_A^Z(Q^2)\gamma^\mu\gamma_5]u(p_1)}$$

(Anti)Neutrino-Nucleon Neutral Current Scattering

★ **Differential cross section:**

$$\frac{d\sigma}{dQ^2} = \frac{G_F^2}{2\pi}\frac{Q^2}{E_\nu^2}(A \pm BW + CW^2)$$

$$\boxed{W = 4(E_\nu/M_p - \tau)}$$

$$\boxed{\tau = \frac{Q^2}{4M_P^2}}$$

$$\boxed{A = \tfrac{1}{4}\{(G_A^Z)^2(1+\tau) - [(F_1^Z)^2 - \tau(F_2^Z)^2](1-\tau) + 4\tau F_1^Z F_2^Z\}}$$

$$\boxed{B = -\tfrac{1}{4}G_A^Z(F_1^Z + F_2^Z)}$$

$$\boxed{C = \frac{1}{64\tau}[(G_A^Z)^2 + (F_1^Z)^2 + \tau(F_2^Z)^2]}$$

Neutral weak Dirac & Pauli FFs

Neutral weak axial FF

★ Neutral current matrix elements

$$F_i^{ZN} = \pm\frac{1}{2}\left(F_i^p - F_i^n\right) - 2\,\sin^2\vartheta_{\mathrm{W}}\,F_i^N - \frac{1}{2}\,F_i^{sN} \qquad (i = 1, 2;\ N = p, n)$$

Strange quark Dirac and Pauli form factors
not constrained from e-p parity-violating scattering (PVES)

$$G_i^{ZN}(Q^2) = \pm\frac{1}{2}\,G_i(Q^2) - \frac{1}{2}\,G_i^{sN}(Q^2) \qquad (i = A, P;\ N = p, n)$$

Neutral weak axial FF
unknown radiative
correction in PVES

Iso-vector axial FF
not constrained from
CCQE scattering

Strange quark axial FF
Q^2 behavior - not constrained

Lattice QCD Calculation of Nucleon FFs

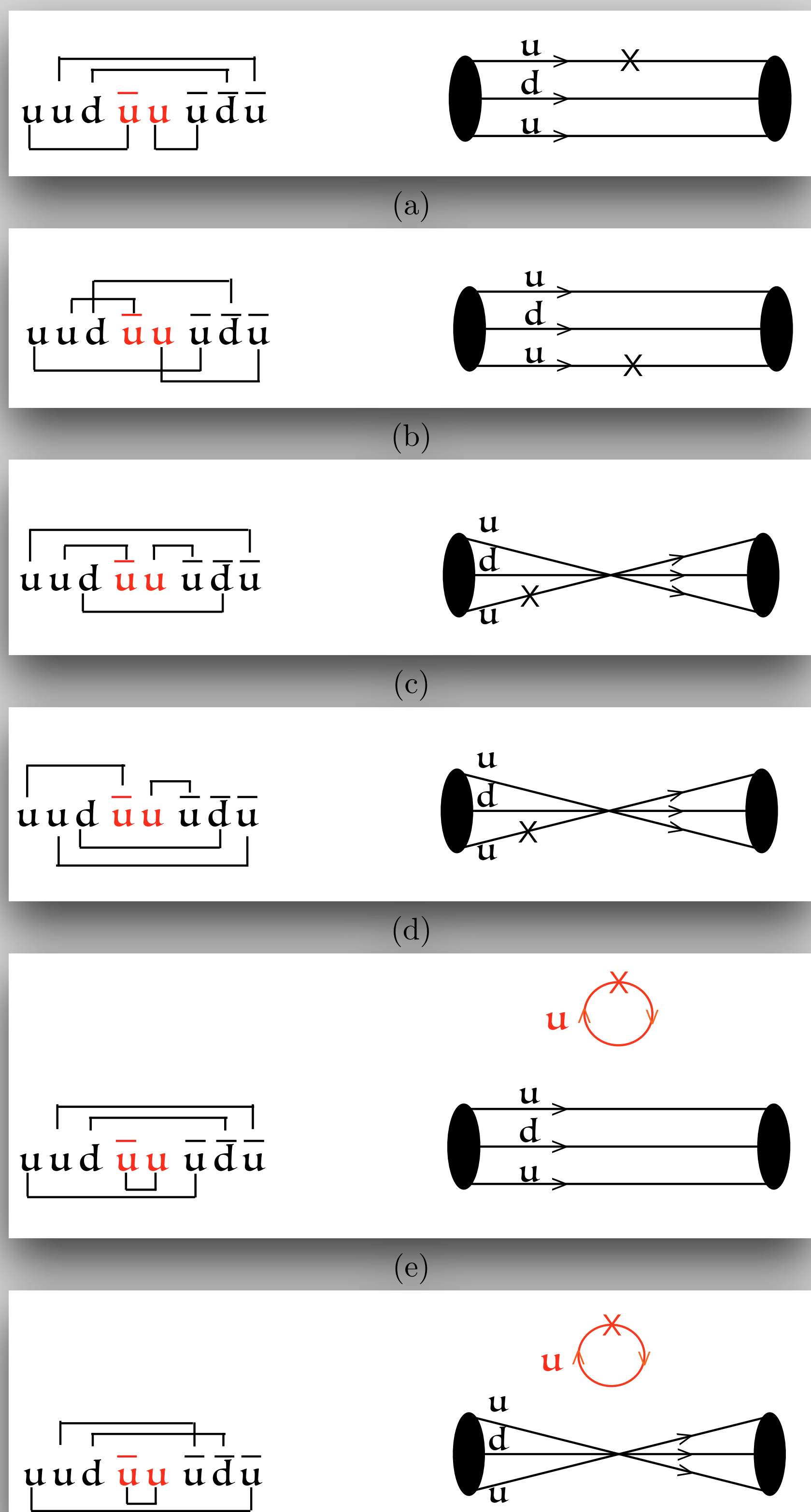

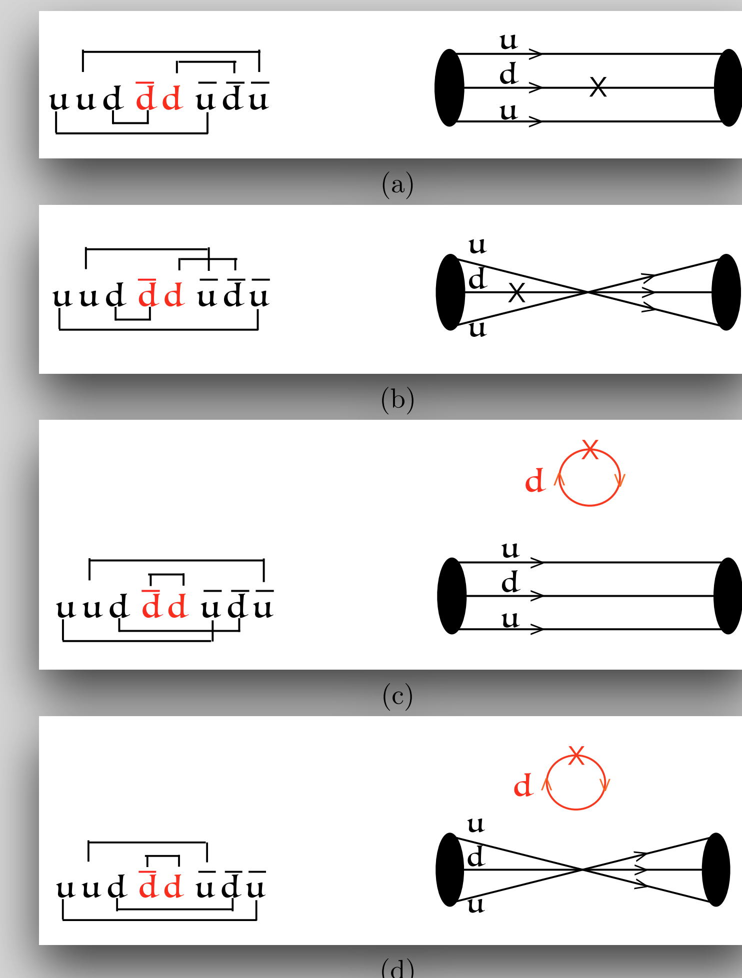

Self contracted sea-quark loop correlated with valence quarks in the nucleon propagator by fluctuating background gauge fields

★ Obtain matrix element from suitable ratio of 3-point to 2-point functions

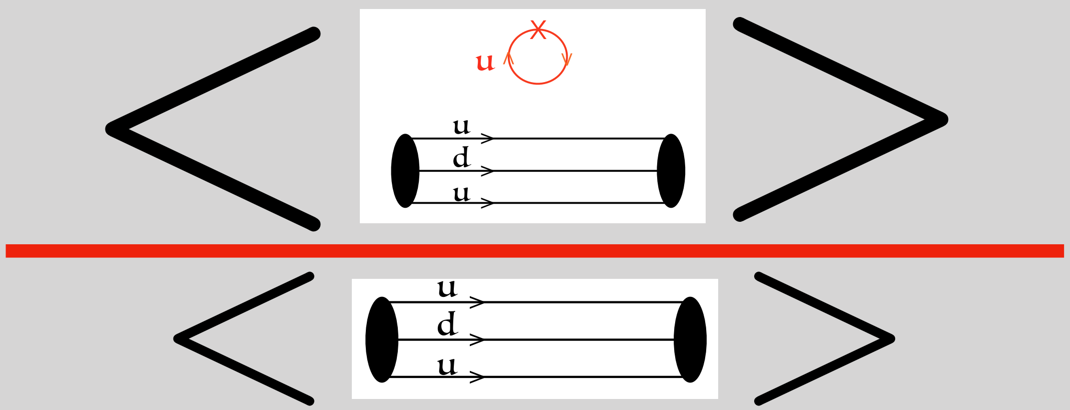

★ Perform a two-states fit,

$$R(t_1, t_2) = C_0 + C_1 e^{-\delta m (t_2 - t_1)} + C_2 e^{-\delta m t_1}$$

★ *With better statistics, one can perform multiple states fit*

Lattice QCD Calculation of Nucleon FFs

★ Example two-states fit

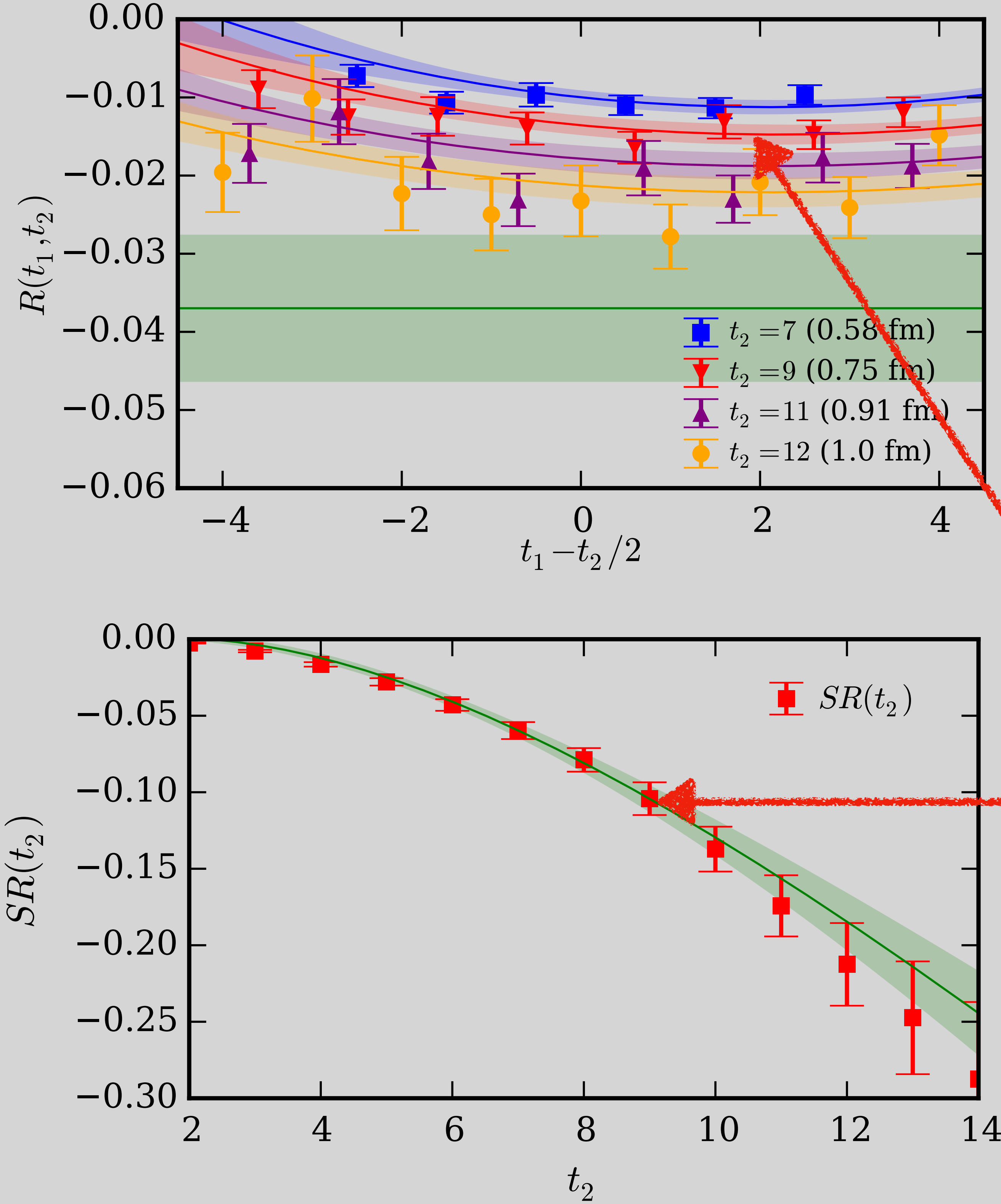

Ratio

Summed Ratio

Towards Lattice QCD Calculation of Neutral Weak FFs

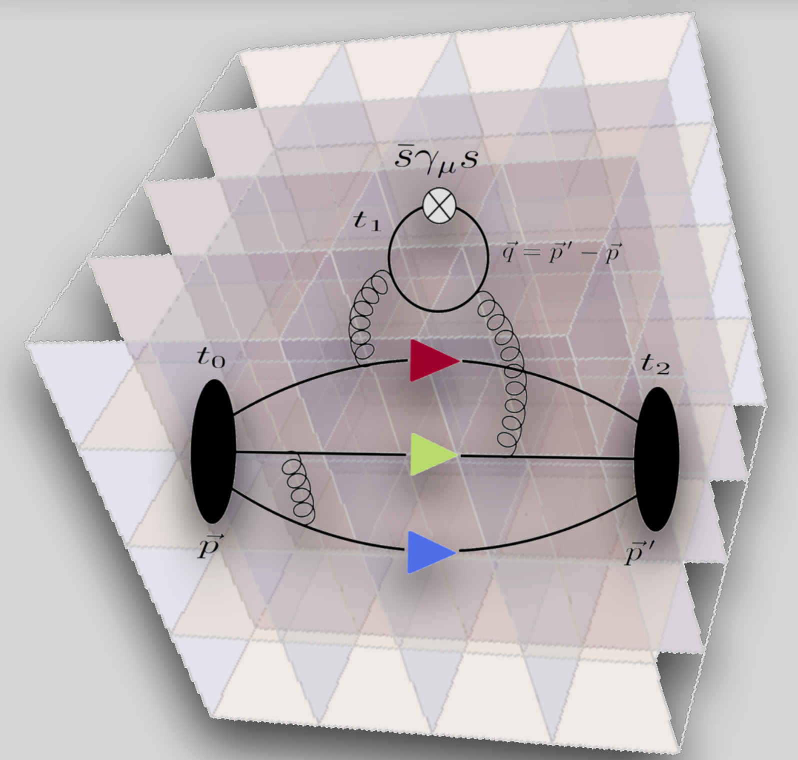

Overlap fermion on RBC/UKQCD DWF

$L^3 \times T$	a (fm)	$m_s^{(s)}$(MeV)	m_π (MeV)	N_{config}
$24^3 \times 64$	0.1105(3)	120	330	203
$32^3 \times 64$	0.0828(3)	110	300	309
$48^3 \times 96$	0.1141(2)	94.9	139	81
$32^3 \times 64$	0.1431(7)	89.4	171	200

$$G_M^{s,z-exp}(Q^2) = \sum_{k=0}^{k_{\max}} a_k z^k$$

$$z = \frac{\sqrt{t_{\text{cut}} + Q^2} - \sqrt{t_{\text{cut}}}}{\sqrt{t_{\text{cut}} + Q^2} + \sqrt{t_{\text{cut}}}}$$

Perform z-expansion to perform Q^2 fit
Richard Hill, et. al 2010

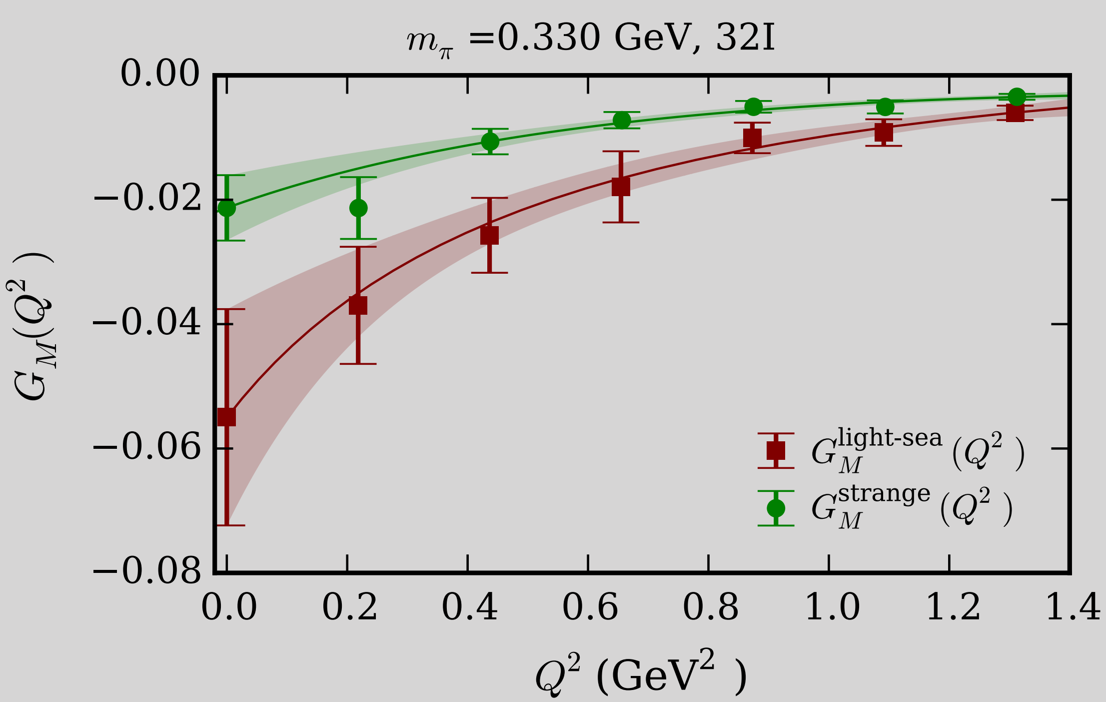

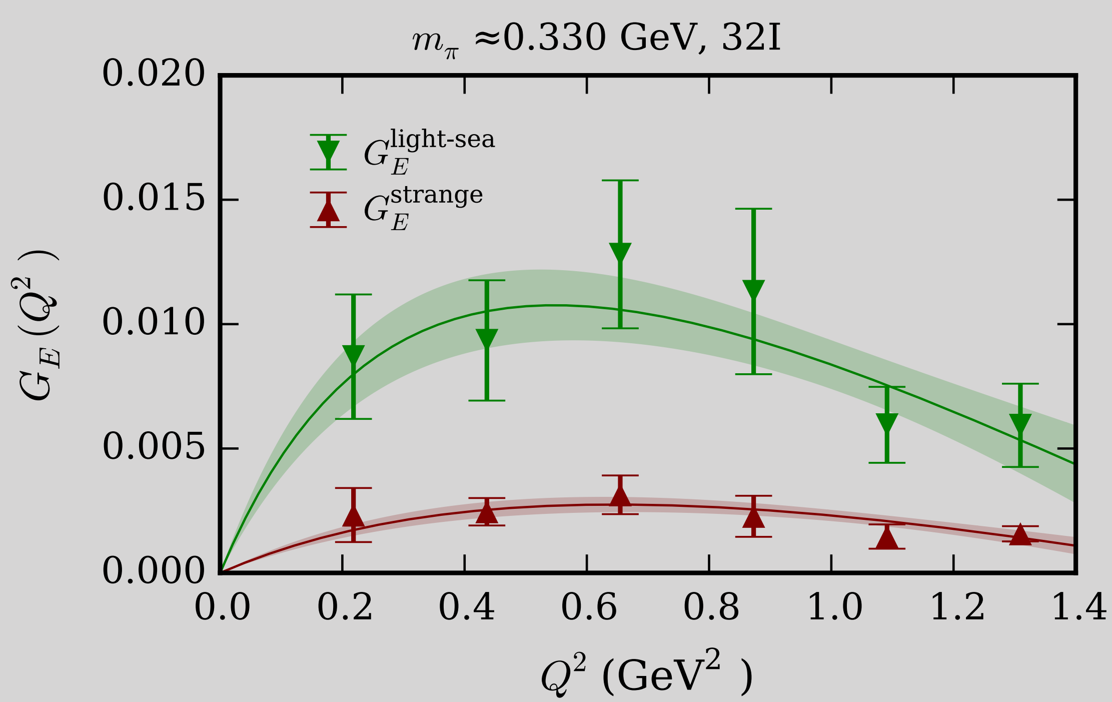

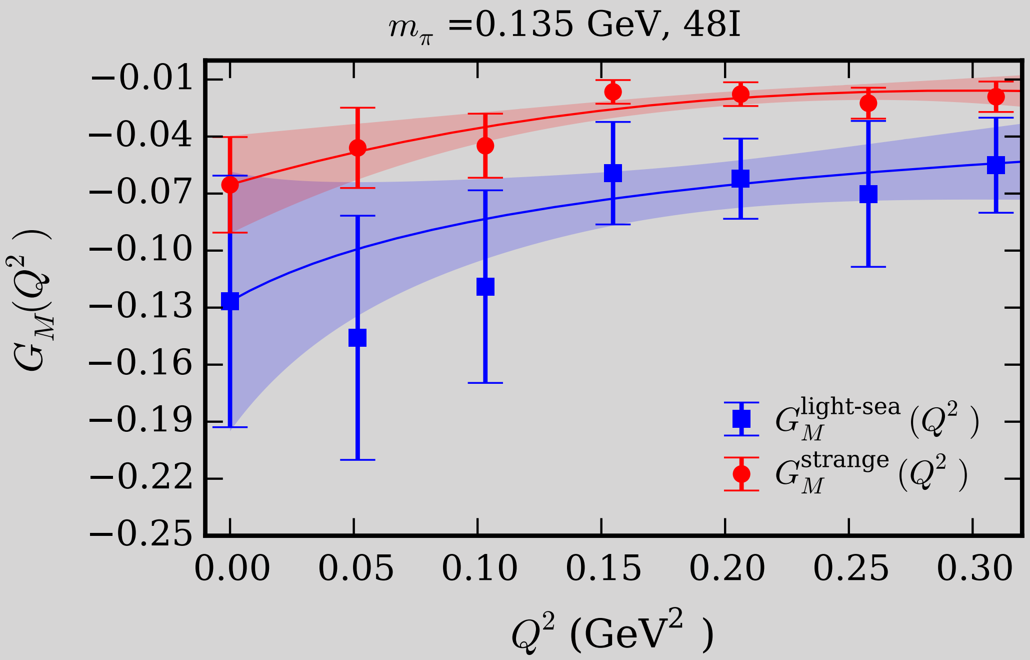

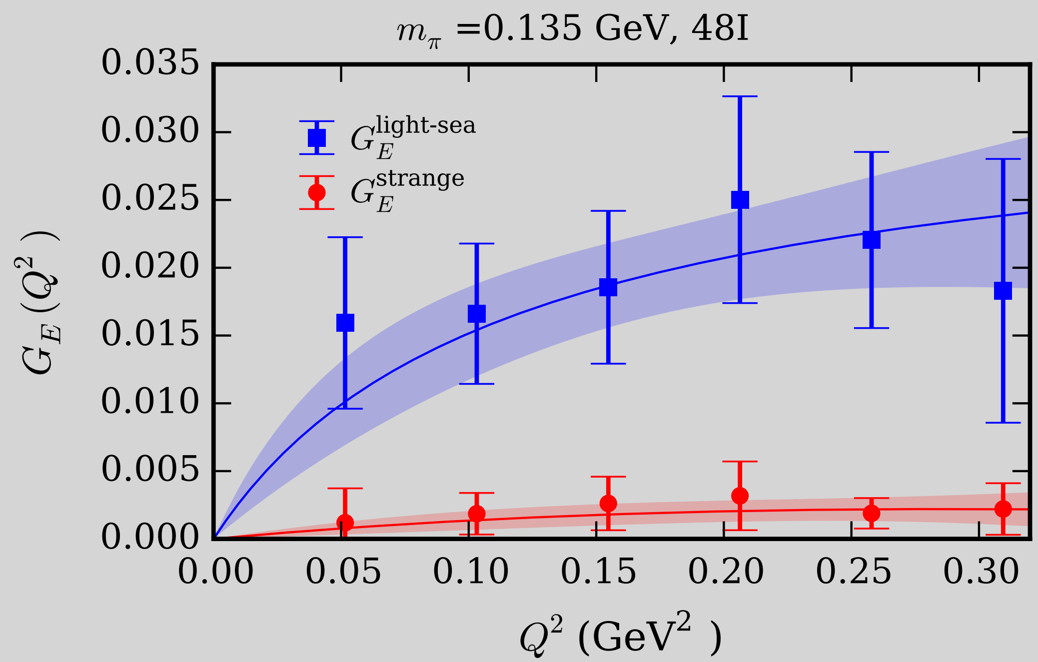

FF at each Q^2 obtained through *z-expansion* and using 24 data points in a simultaneous chiral, continuum, and infinite volume extrapolation

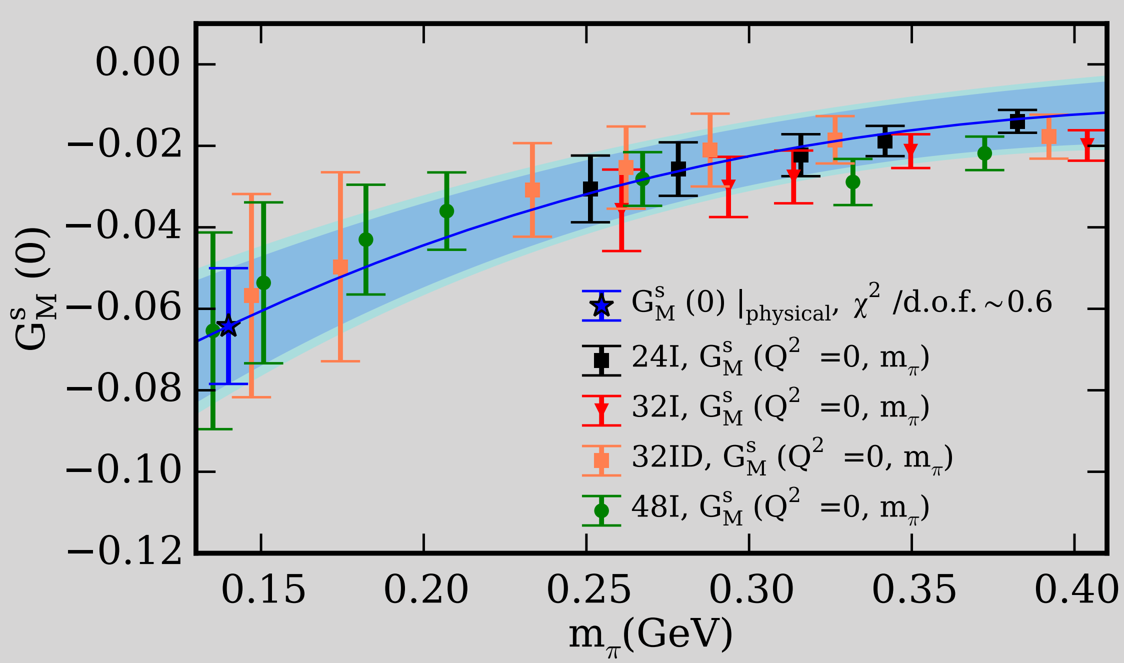

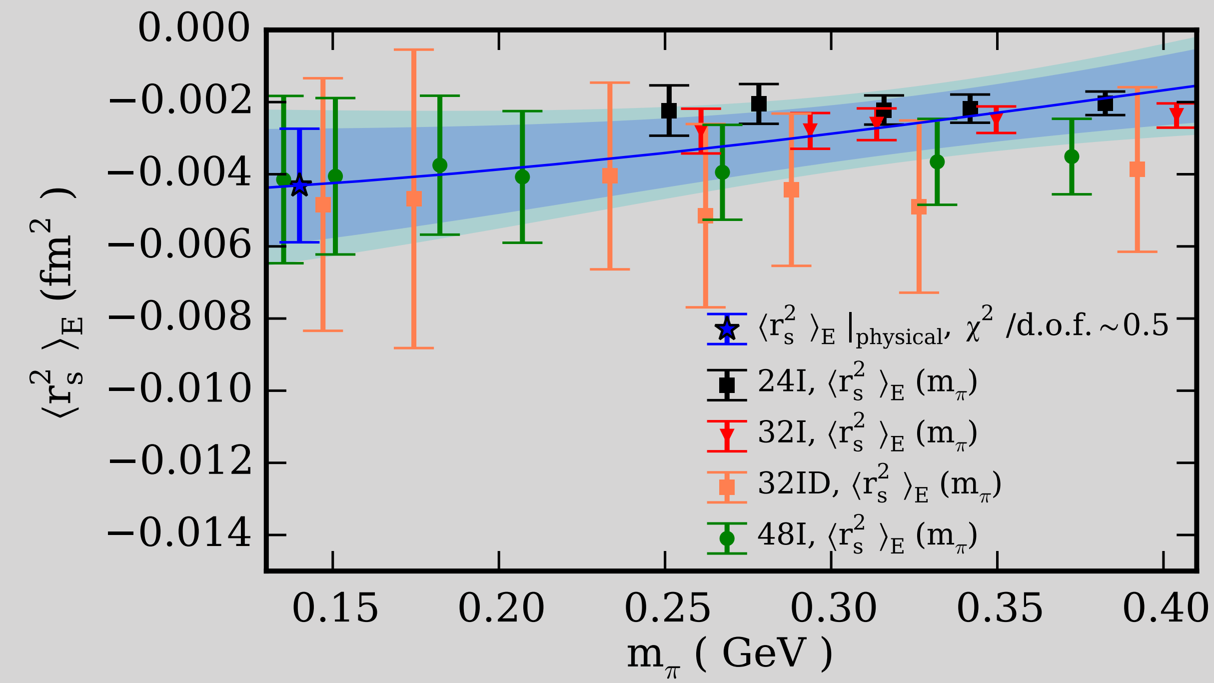

$$G_M^s(0)|_{\text{physical}} = -0.064(14)(04)(06)(06)$$

$$\langle r_s^2\rangle_E|_{\text{physical}} = -0.0043(16)(02)(08)(07)\,\text{fm}^2$$

RSS, Yang, et. al. PRL 118, 2017

Strange quark FF

RSS, PRD 2017

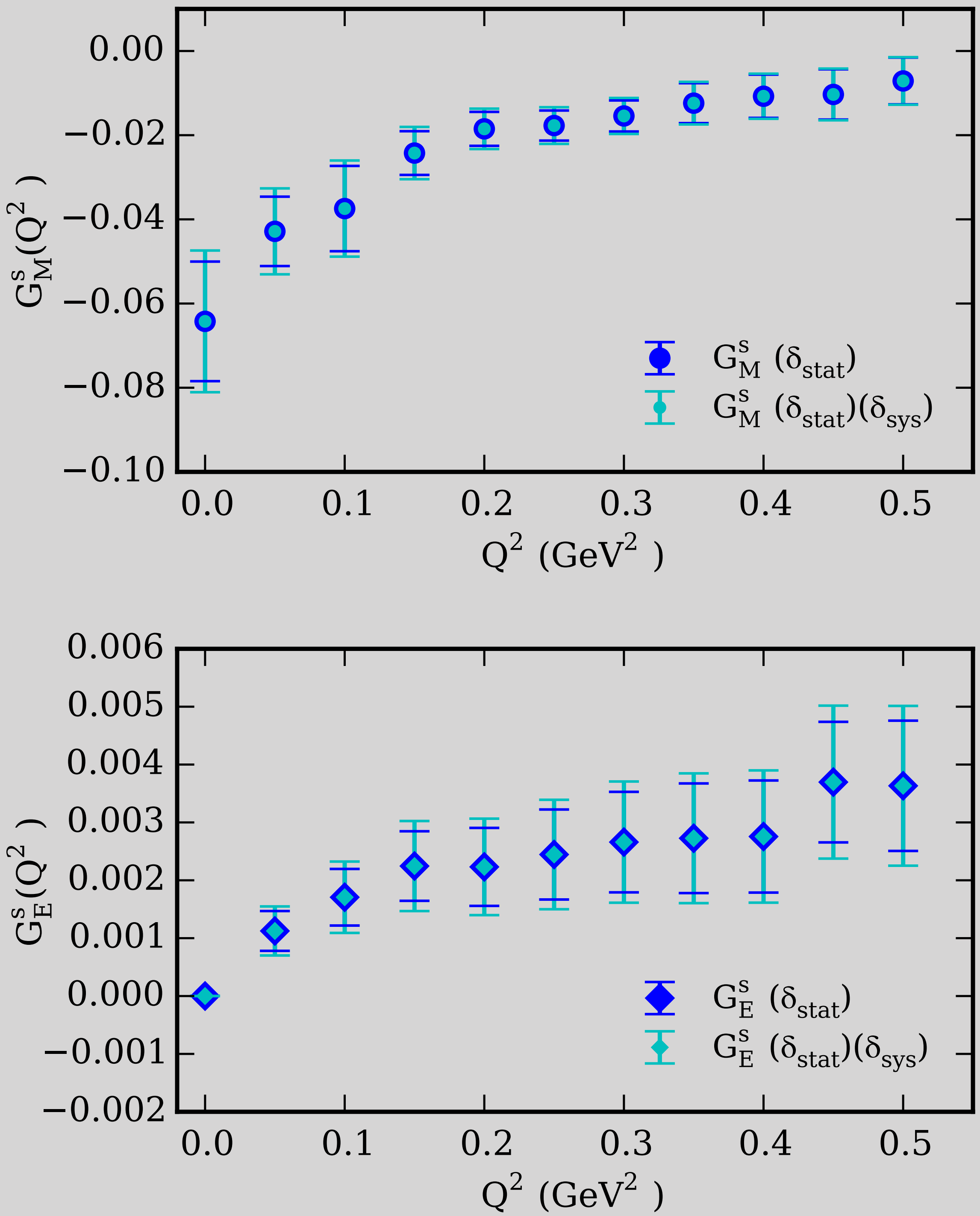

Nucleon-sea u, d quark FF

RSS, Yang, et. al. PRD 2017

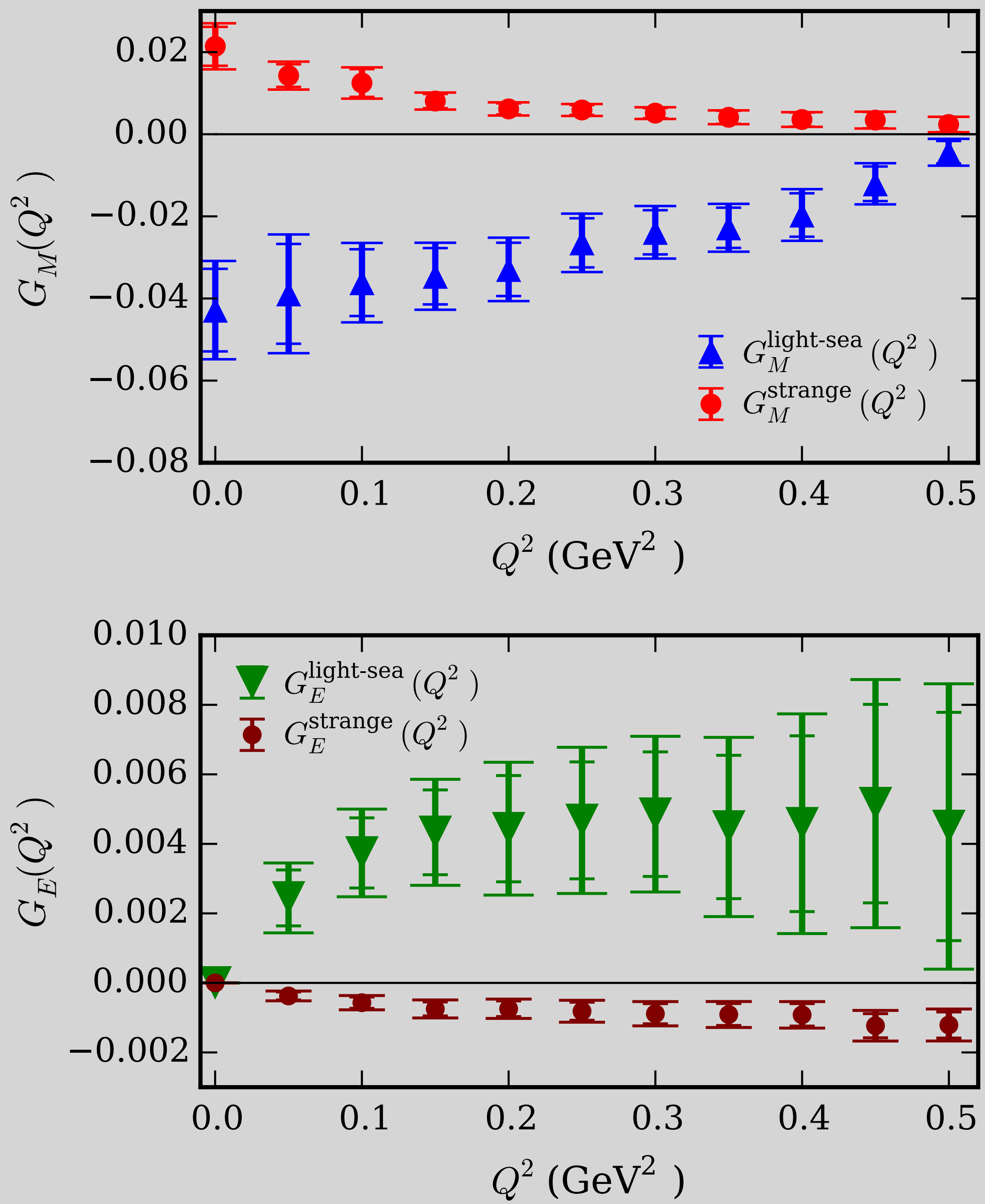

Charge factors included

Neutral Weak FFs

$$G_{E,M}^{Z,p(n)}(Q^2) = \frac{1}{4}\Big[(1-4\sin^2\theta_W)(1+R_V^{p(n)})G_{E,M}^{\gamma,p(n)}(Q^2) - (1+R_V^{n(p)})G_{E,M}^{\gamma,n(p)}(Q^2) - (1+R_V^{(0)})G_{E,M}^{s}(Q^2)\Big]$$

★ Lattice QCD input for strange FF

★ Phenomenological input for nucleon EMFF → **RSS, de Teramond, Brodsky, Dosch, Deur PRD 2017**

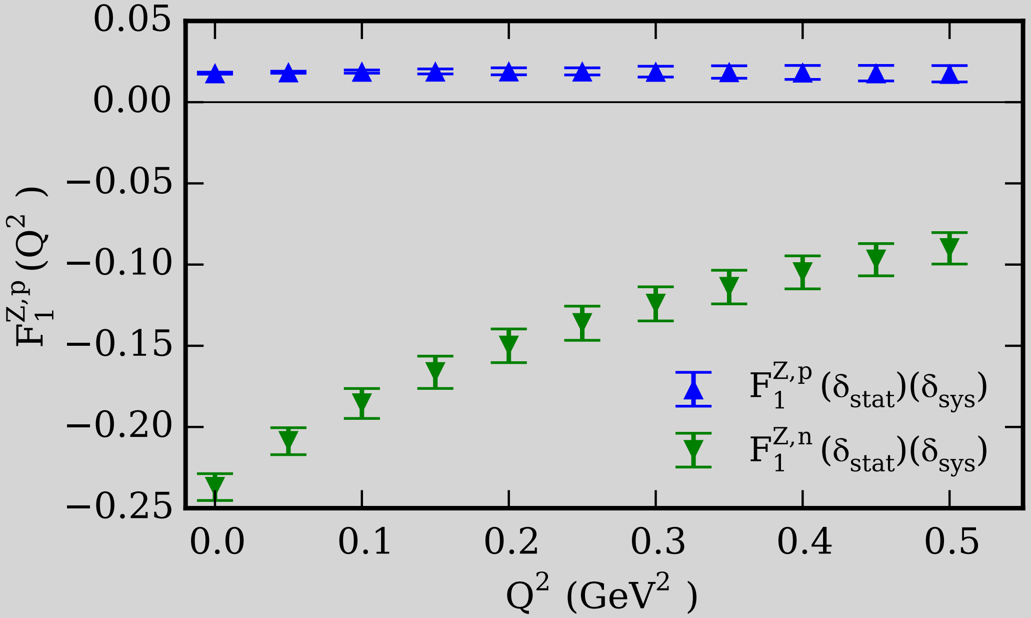

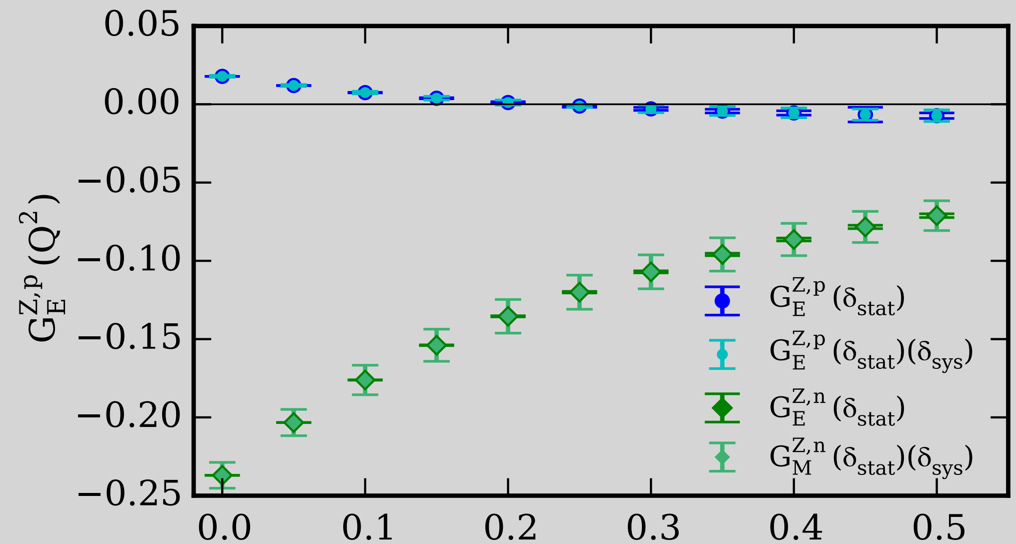

$$F_i^{ZN} = \pm\frac{1}{2}(F_i^p - F_i^n) - 2\sin^2\vartheta_W F_i^N - \frac{1}{2}F_i^{sN} \qquad (i=1,2;\ N=p,n)$$

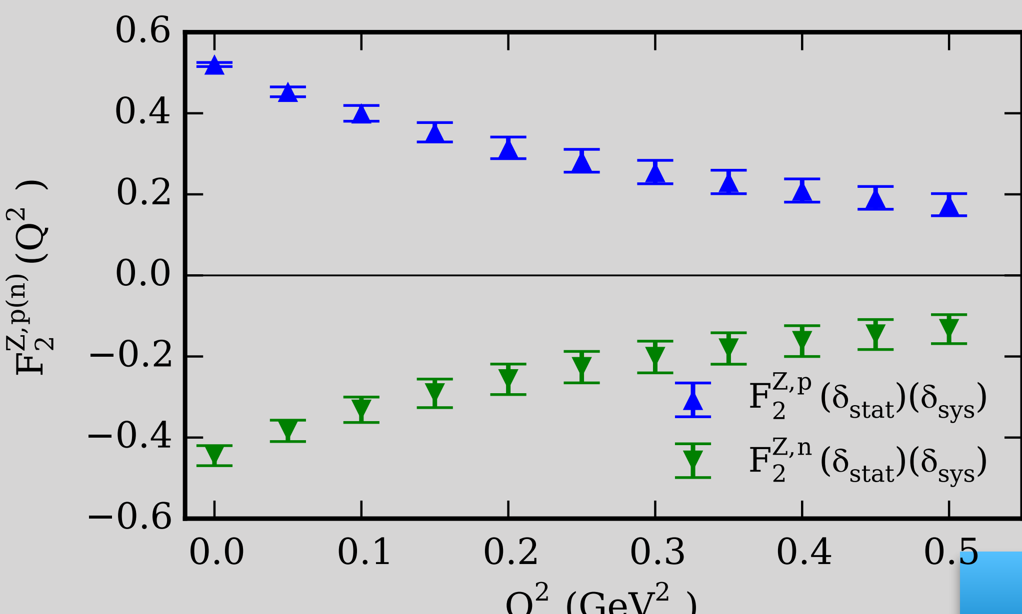

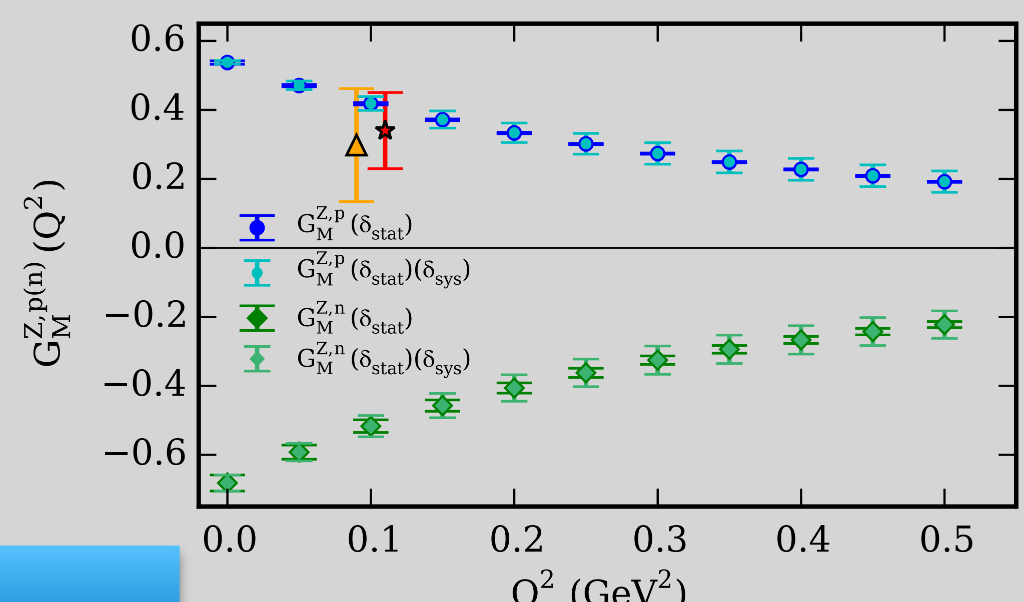

RSS PRD 96, 093007 (2017)

Why Neutral Current FFs are Challenging to Measure in PVES Experiment

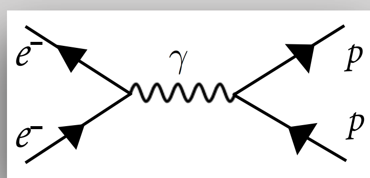

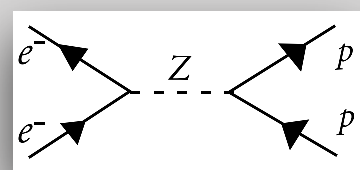

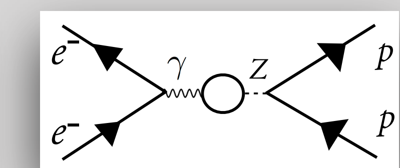

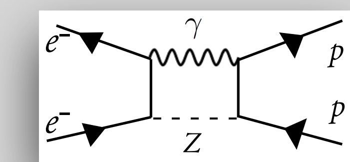

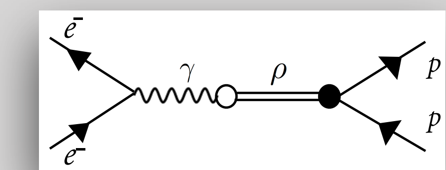

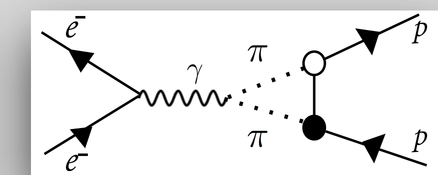

Zel'dovich (58)
Kaplan, Manohar (88)
McKeown, Beck (89)

$$\mathcal{M}_Z = \frac{G_F}{2\sqrt{2}}(g_V^i l^\mu + g_A^i l^{\mu 5})(J_\mu^Z + J_{\mu 5}^Z)$$

$$\mathcal{M}_Z^{PV} = \frac{G_F}{2\sqrt{2}}(g_V^i l^\mu J_{\mu 5}^Z + g_A^i l^{\mu 5} J_\mu^Z)$$

$$\mathcal{M}_Z^{PC} = \frac{G_F}{2\sqrt{2}}(g_V^i l^\mu J_\mu^Z + g_A^i l^{\mu 5} J_{\mu 5}^Z)$$

$\epsilon' \to 0$ as scattering angle $\to 0$

$$A_{ep} = A_0\left[\frac{\varepsilon G_E^\gamma G_E^Z + \tau G_M^\gamma G_M^Z - (1 - 4\sin^2\theta_W)\varepsilon' G_M^\gamma G_A^Z}{\varepsilon (G_E^\gamma)^2 + \tau (G_M^\gamma)^2}\right]$$

Makes forward scattering experiment less useful

$$(1 - 4\sin^2\theta_W) << 1$$

Suppresses tree-level value
Higher order corrections (unknown) must be considered

Qweak Experiment, Nature 2018

$$G_A^{Z,eff}(0) = -0.59 \pm 0.34$$

Lattice QCD to play the major role to obtain tree-level value and isolate higher order corrections

Lattice QCD Calculation of Proton EMFF

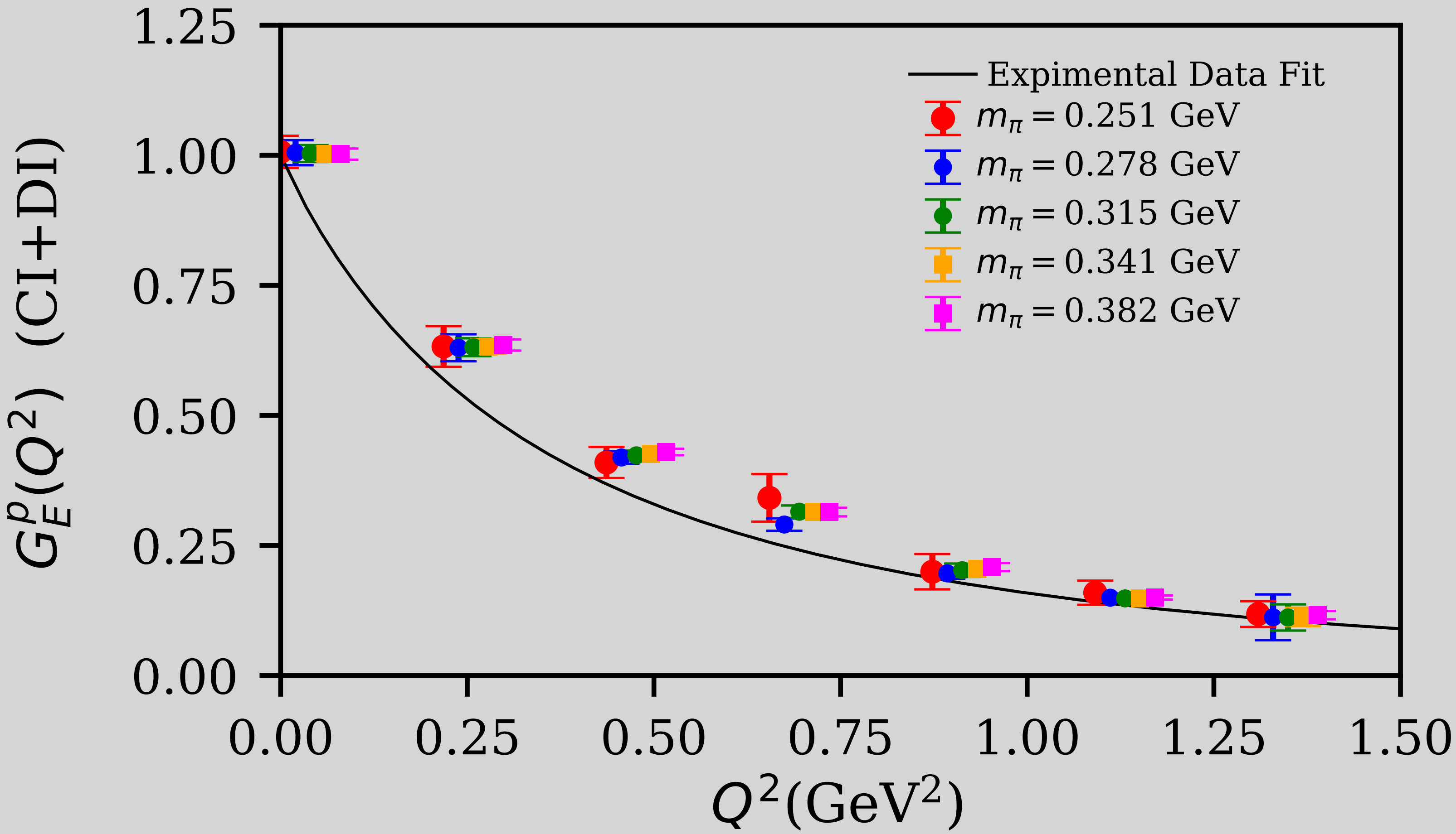

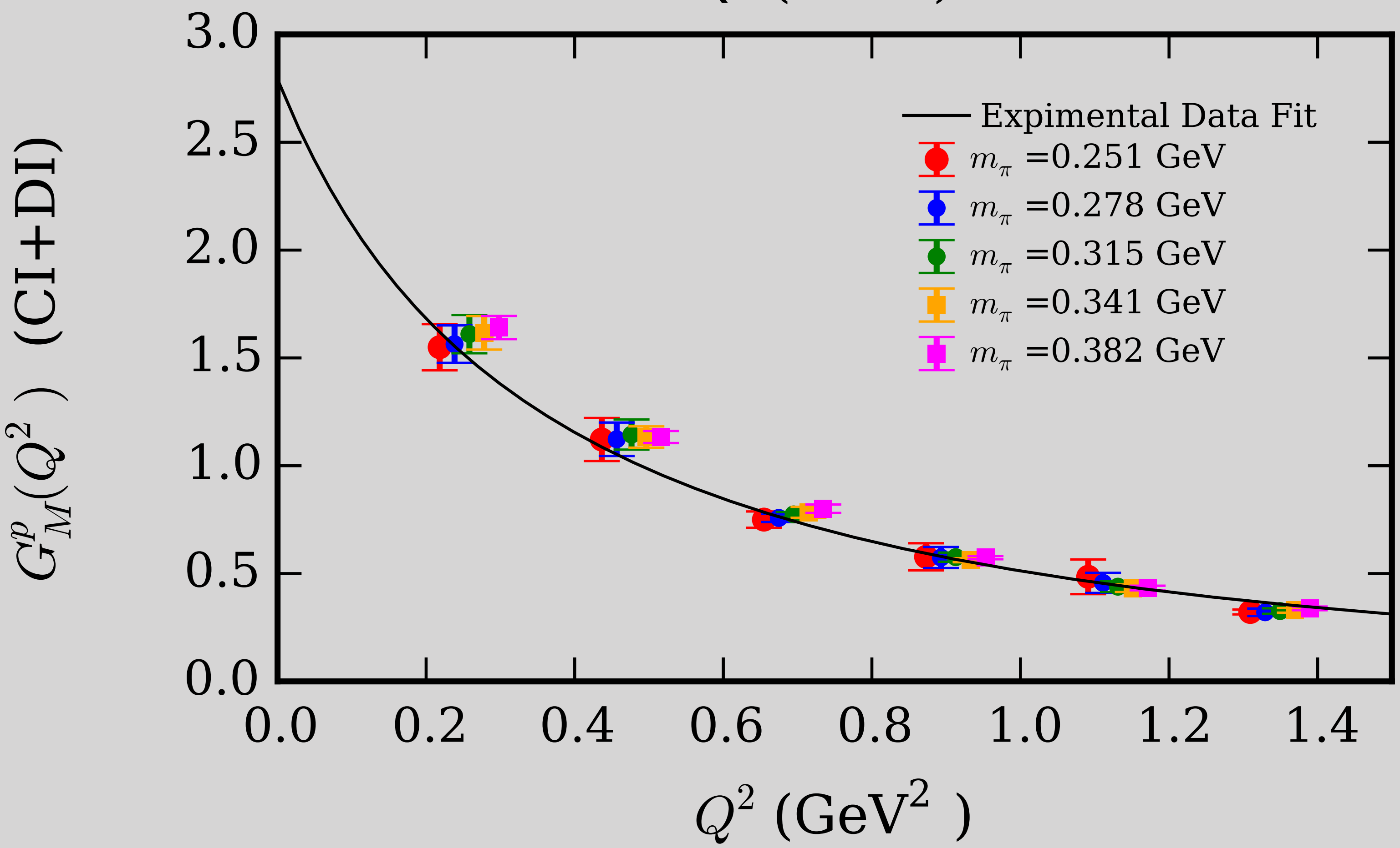

Preliminary

Fit to experimental data
Ye, Arrington, Hill, Lee
PLB 2018

Overlap fermion
on
24I RBC/UKQCD DWF

$$L^3 \times T = 24^3 \times 64$$

$$a = 0.11 \ \text{fm}$$

$$m_\pi = 330 \ \text{MeV}$$

Two-states fit

Lattice QCD Calculation of Neutron EMFF

Preliminary

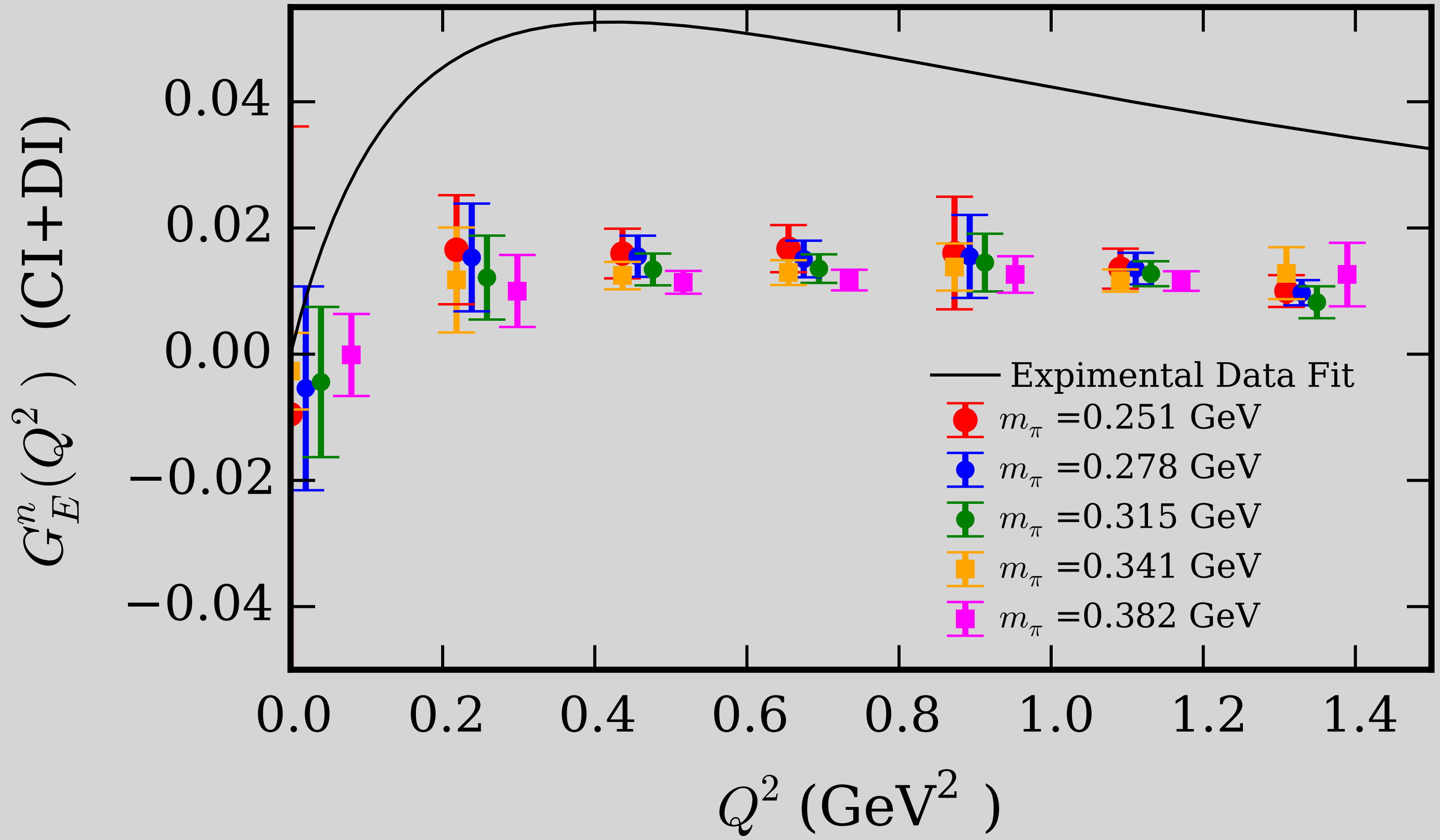

$$L^3 \times T = 24^3 \times 64$$

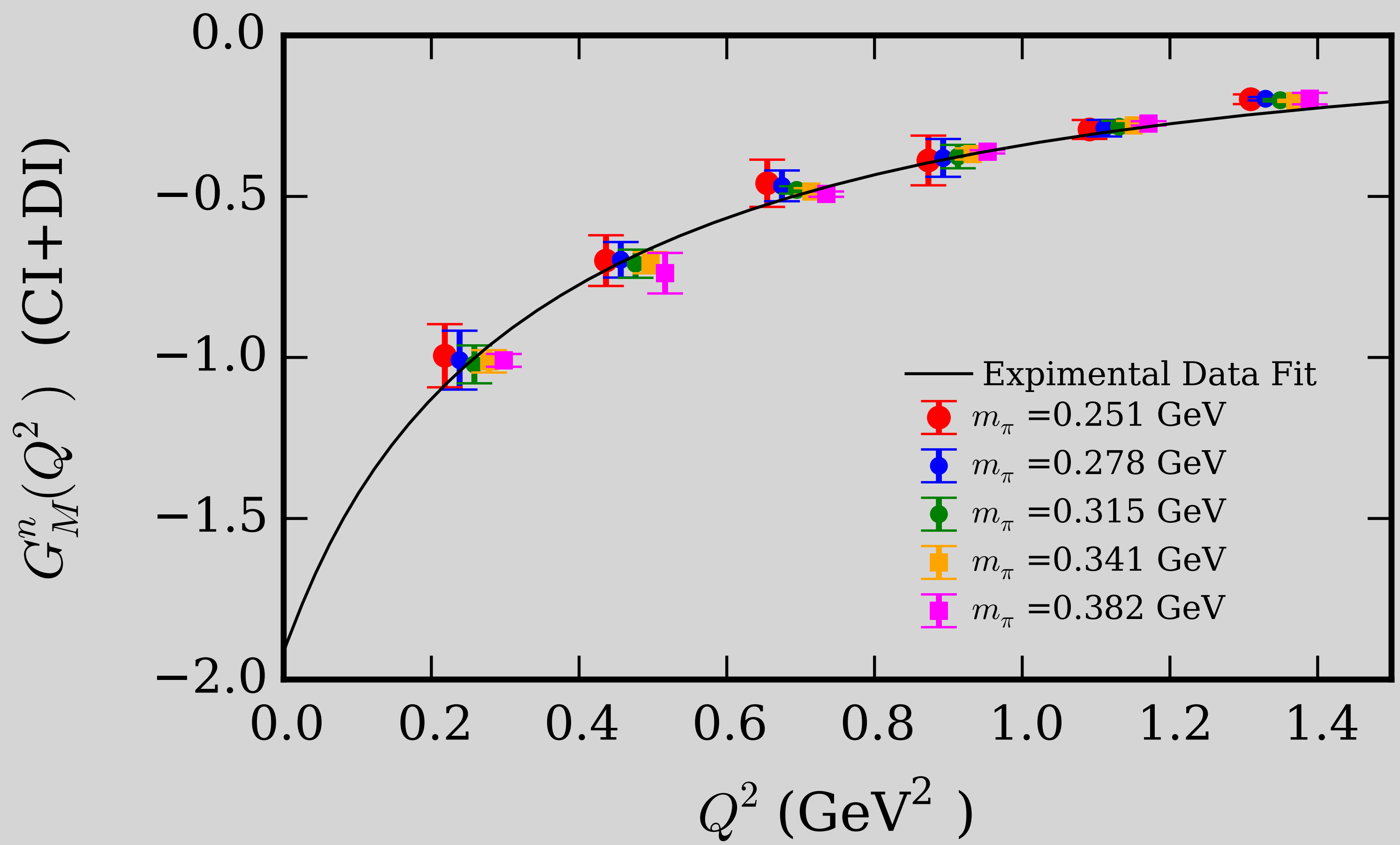

For calculation on 48I DWF
See Lattice 2018 talks
by
Izubuchi & Syritsyn

Lattice QCD Calculation of Proton EMFF

Preliminary

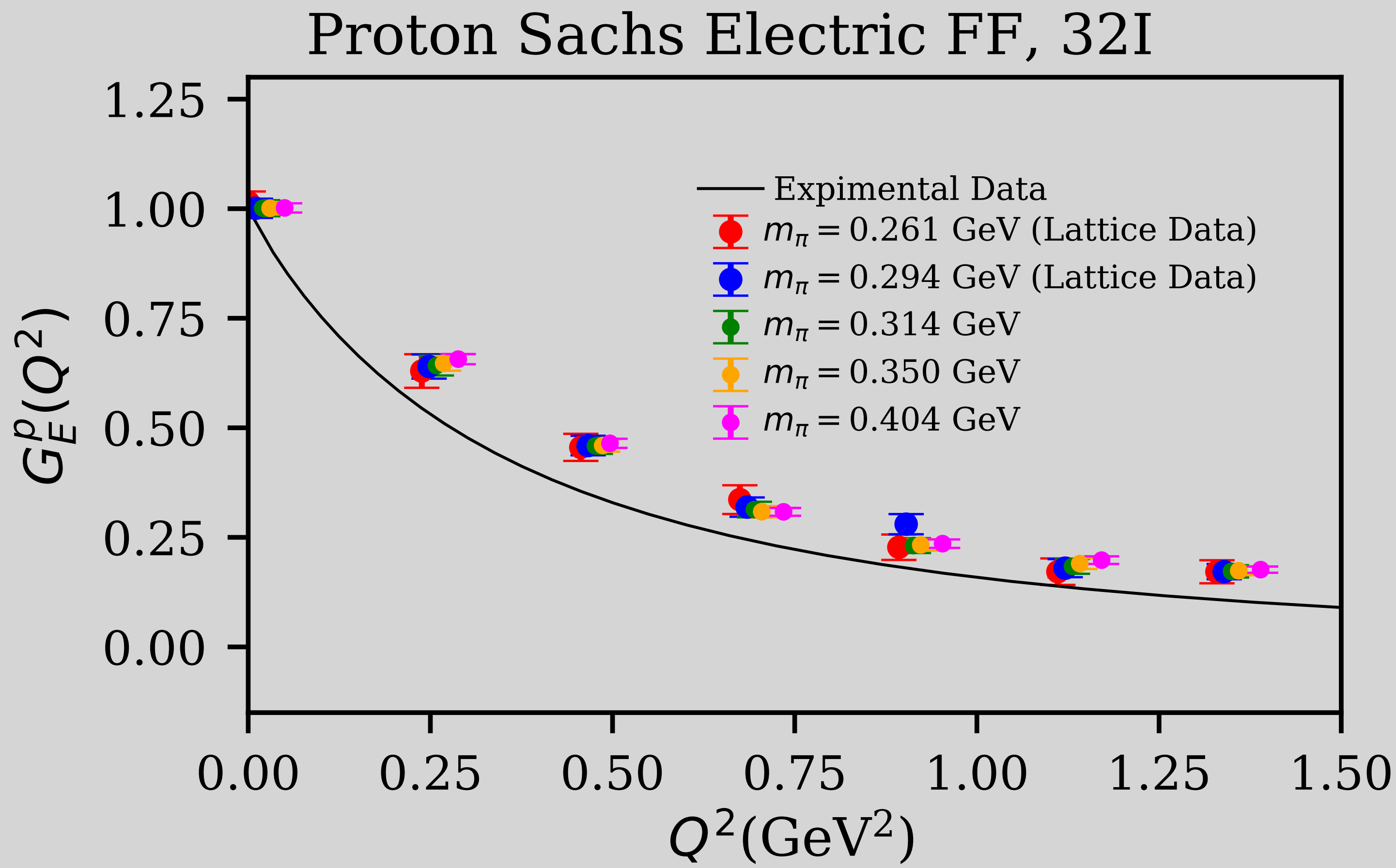

Not a fit yet
average value
from plateau region
of the matrix element
error * 1.5

Sea-quarks contribution
to be added yet

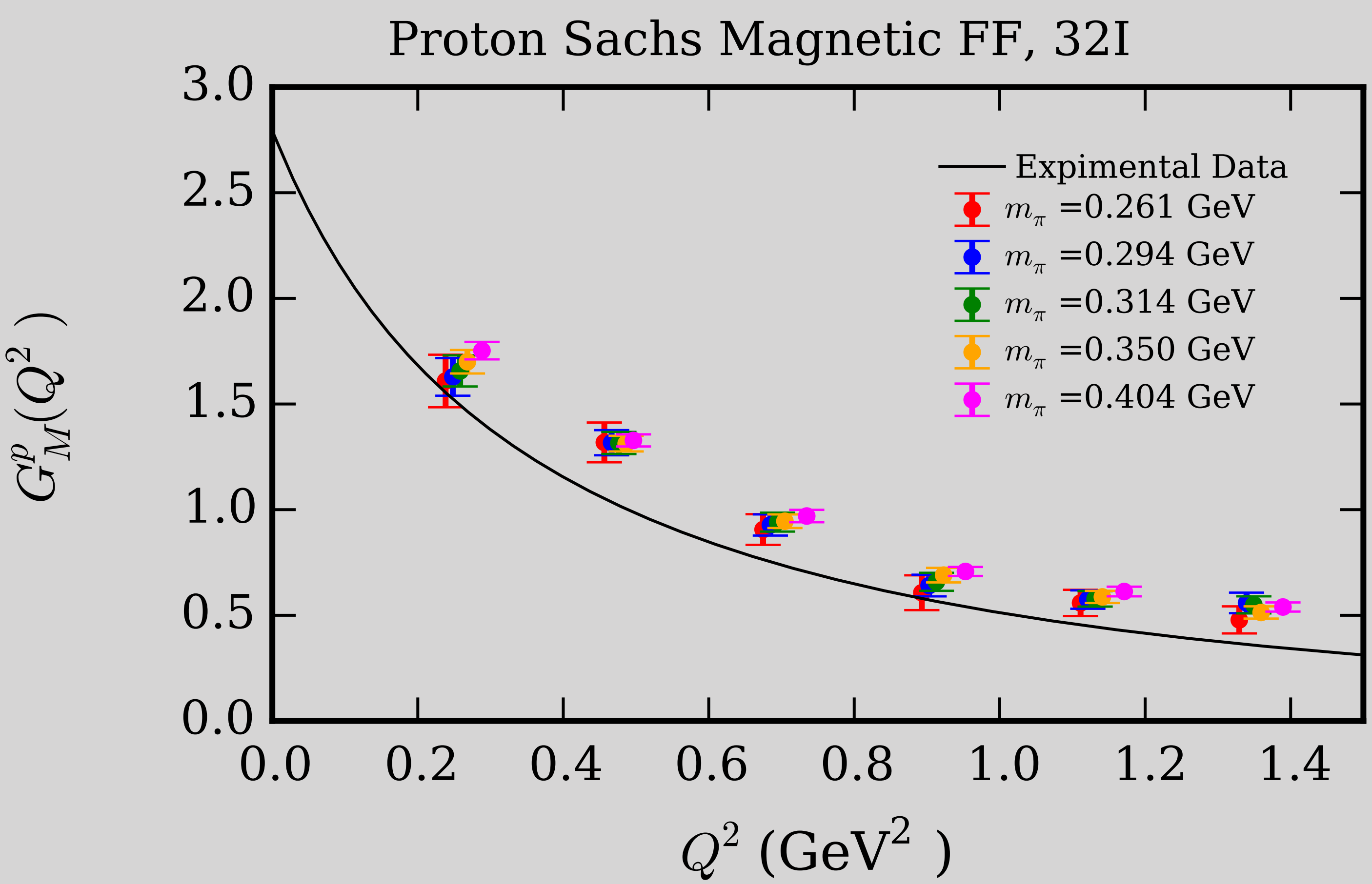

Fit will move the data
Points towards
experimental data fit
and final error will
increase a little

Current Status of Axial Form Factor

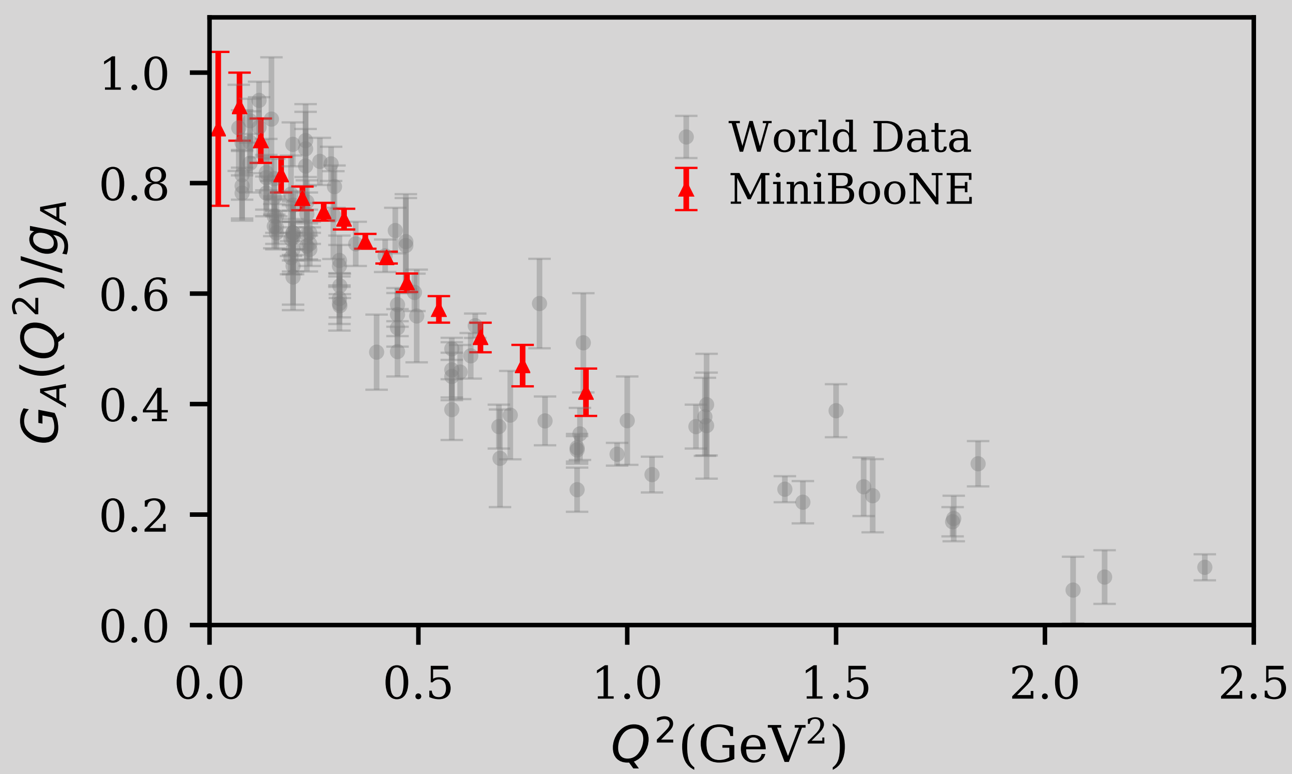

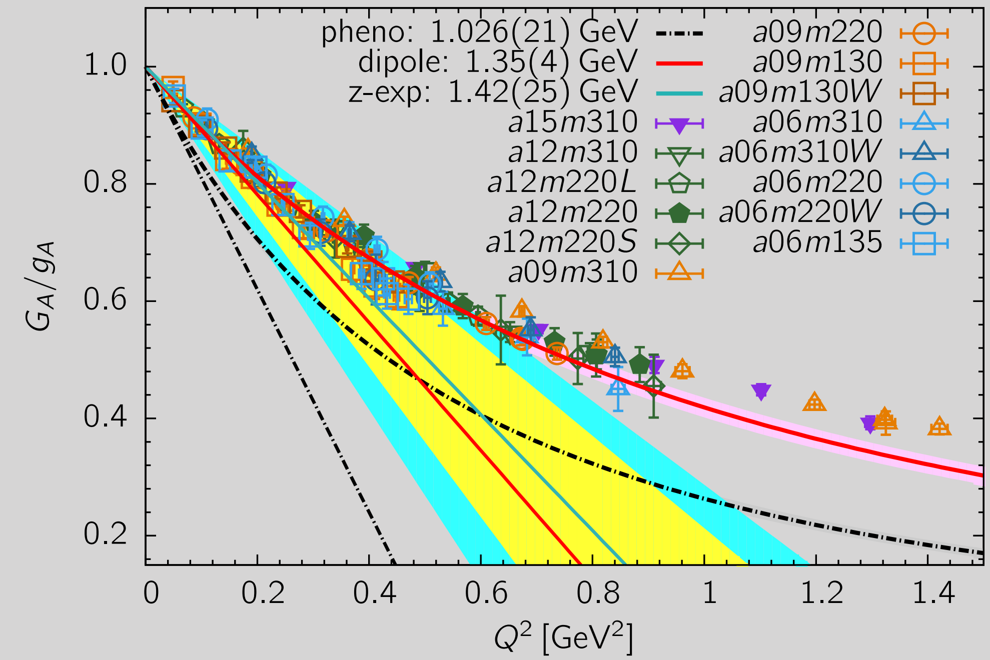

Jang, et. al (PNDME) 2018

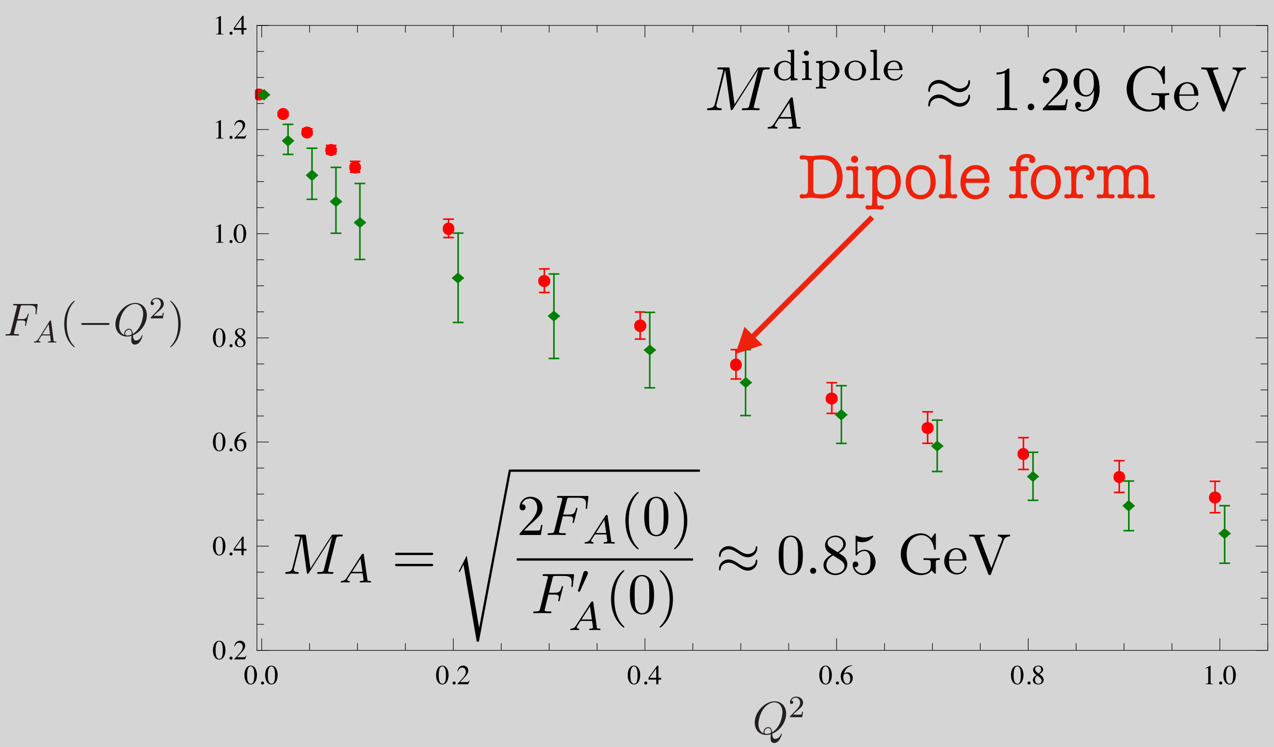

MiniBooNE data
Bhattacharya, Hill, Paz
PRD 2011

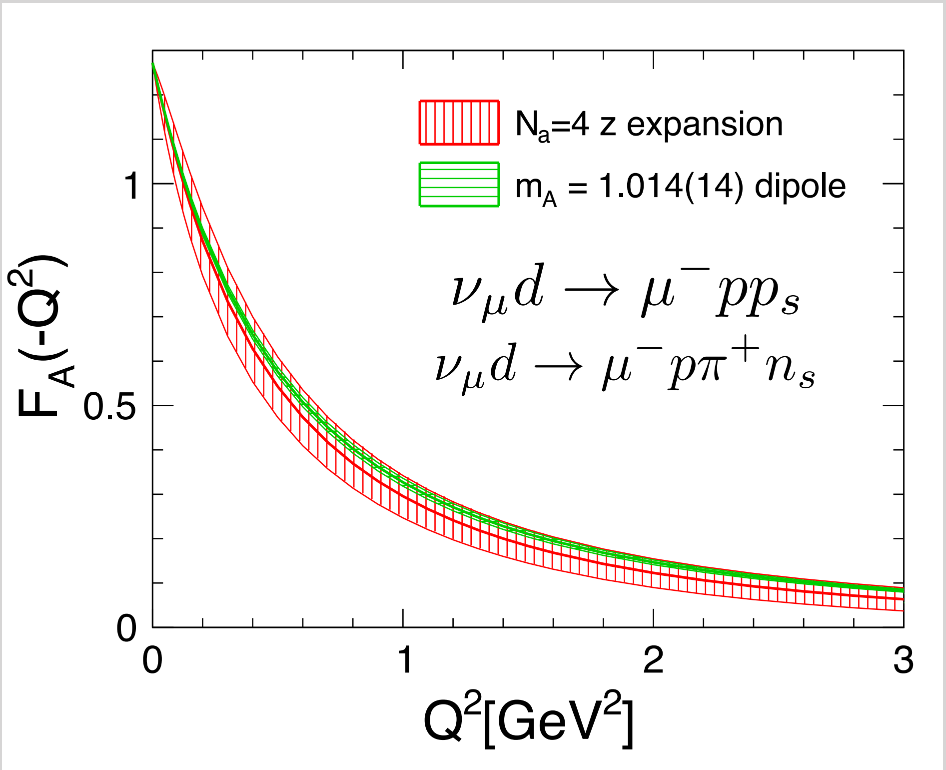

Fit to deuterium target data
Meyer, et. al. PRD 2016

Lattice QCD Calculation of Axial Form Factor

Preliminary

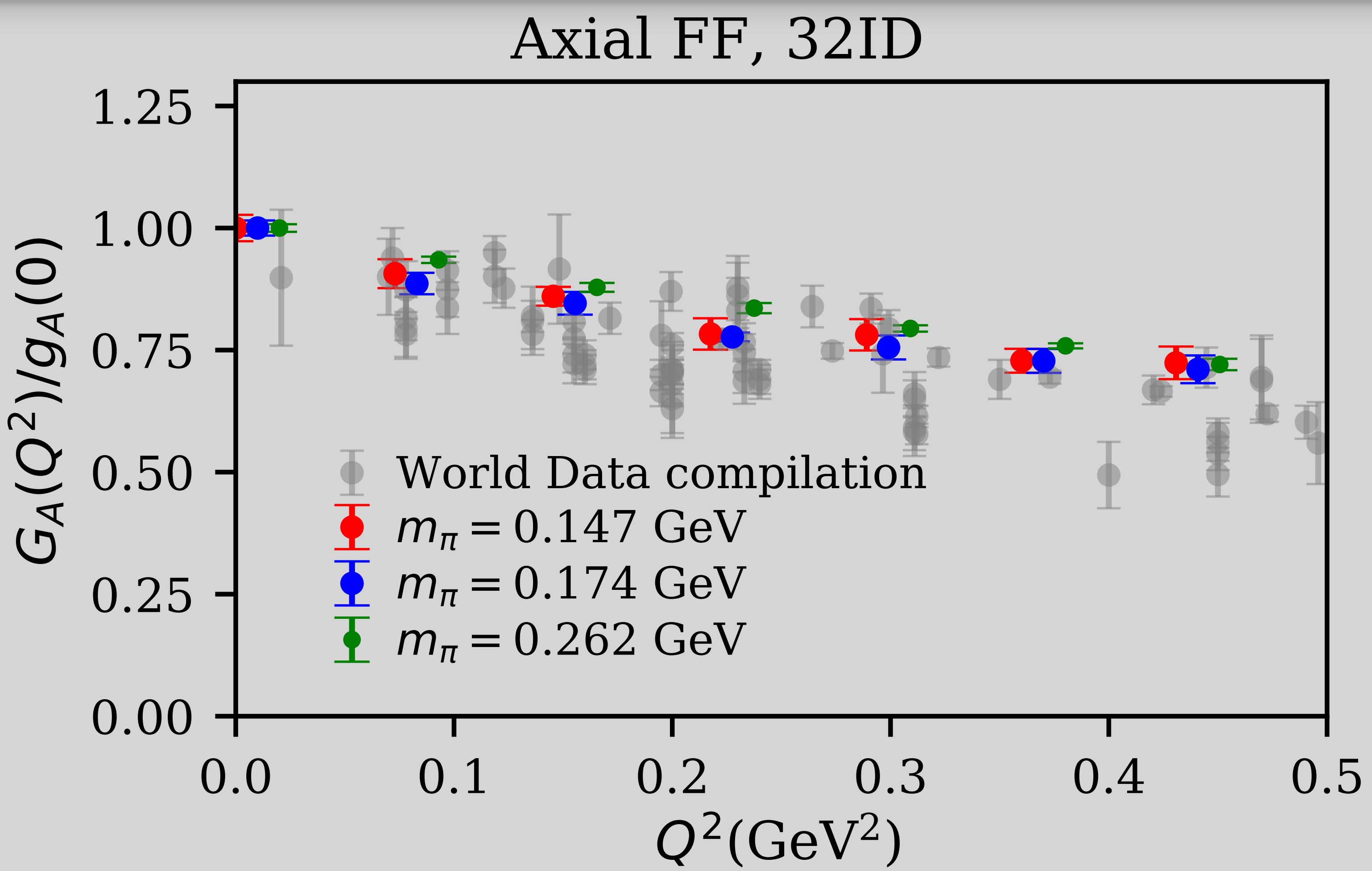

★ Analysis of axial form factor for 4 other pion masses not shown

★ Analysis of nucleon EMFF on 32ID - almost done

★ Producing axial FF data on 24I, 24IDC and 32I lattices

First-principles calculation of (anti)neutrino-nucleon neutral current scattering differential cross sections - to appear in few months

In the meantime, I will proceed with a phenomenological determination of neutral current weak axial form factor $G^Z_A(Q^2)$

Phenomenology: Neutral Current (Anti)Neutrino-Nucleon Scattering

★ Lattice QCD input for strange FF

★ Lattice QCD input for strange quark axial charge

★ Nucleon electromagnetic form factor from z-expansion fit to experimental data from Ye, Arrington, Hill, Lee (PLB 2018)

★ To obtain Q^2 dependence of $G^Z_A(Q^2)$ in a limited region, use MiniBooNE data ($0.25 \lesssim Q^2 \lesssim 0.7 \quad \mathrm{GeV}^2$)

- **Reason 1: Continuum limit lattice $G^s_{E,M}$ uncertainty becomes very large for $Q^2 > 0.7$ GeV^2**

- **Reason 2: Pauli Blocking effect seen to be large for MiniBooNE data at low $Q^2 < 0.20$ GeV^2**

- **Reason 3: Avoid unknown uncertainty associated with detector efficiency correction**

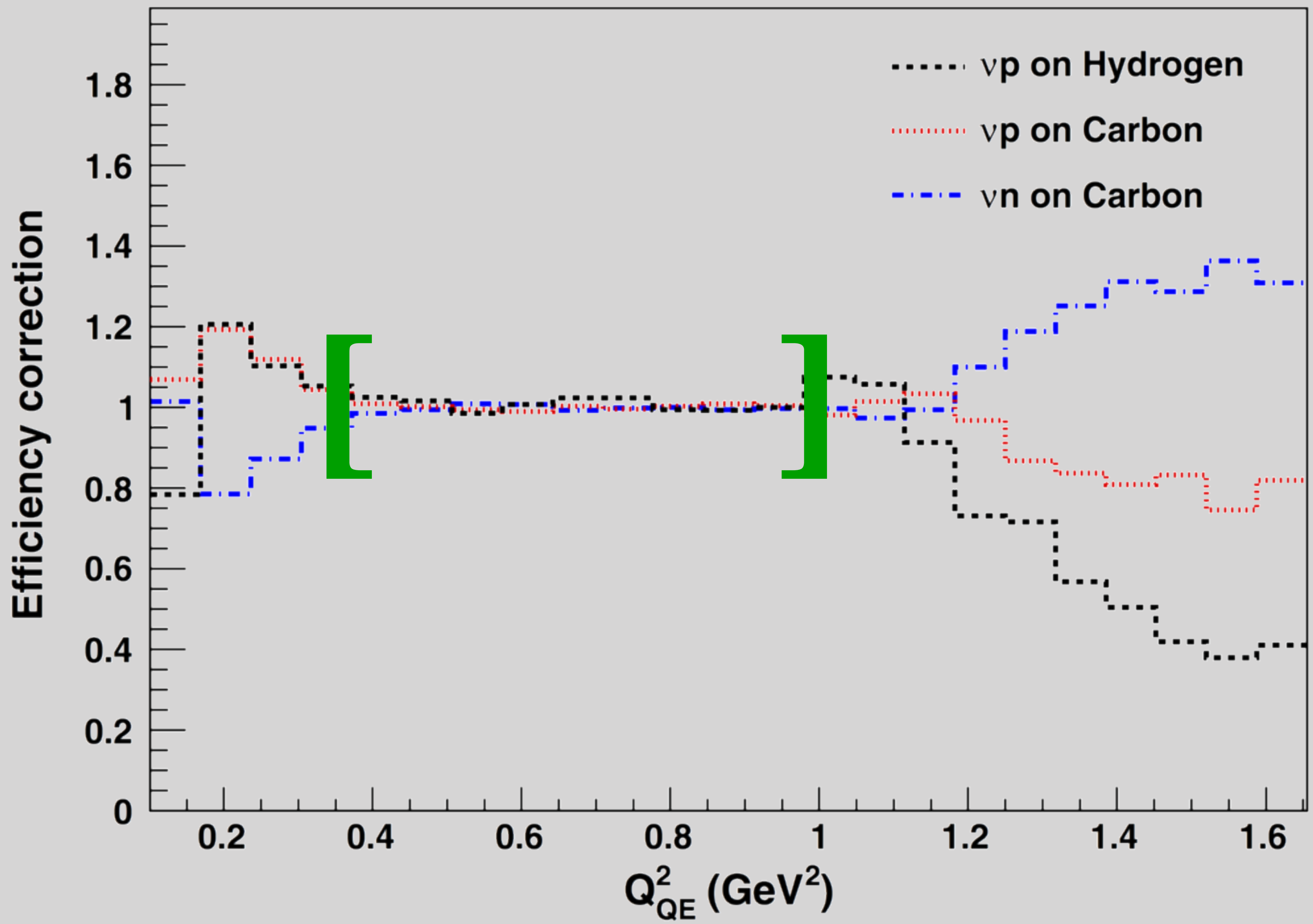

CAUTION: NO ADDITIONAL NUCLEAR EFFECTS CONSIDERED IN THIS ANALYSIS
RELY ON MiniBooNE DATA IN THIS REGION

VALIDITY TEST REQUIRED

Determination of Neutral Current Weak Axial FF

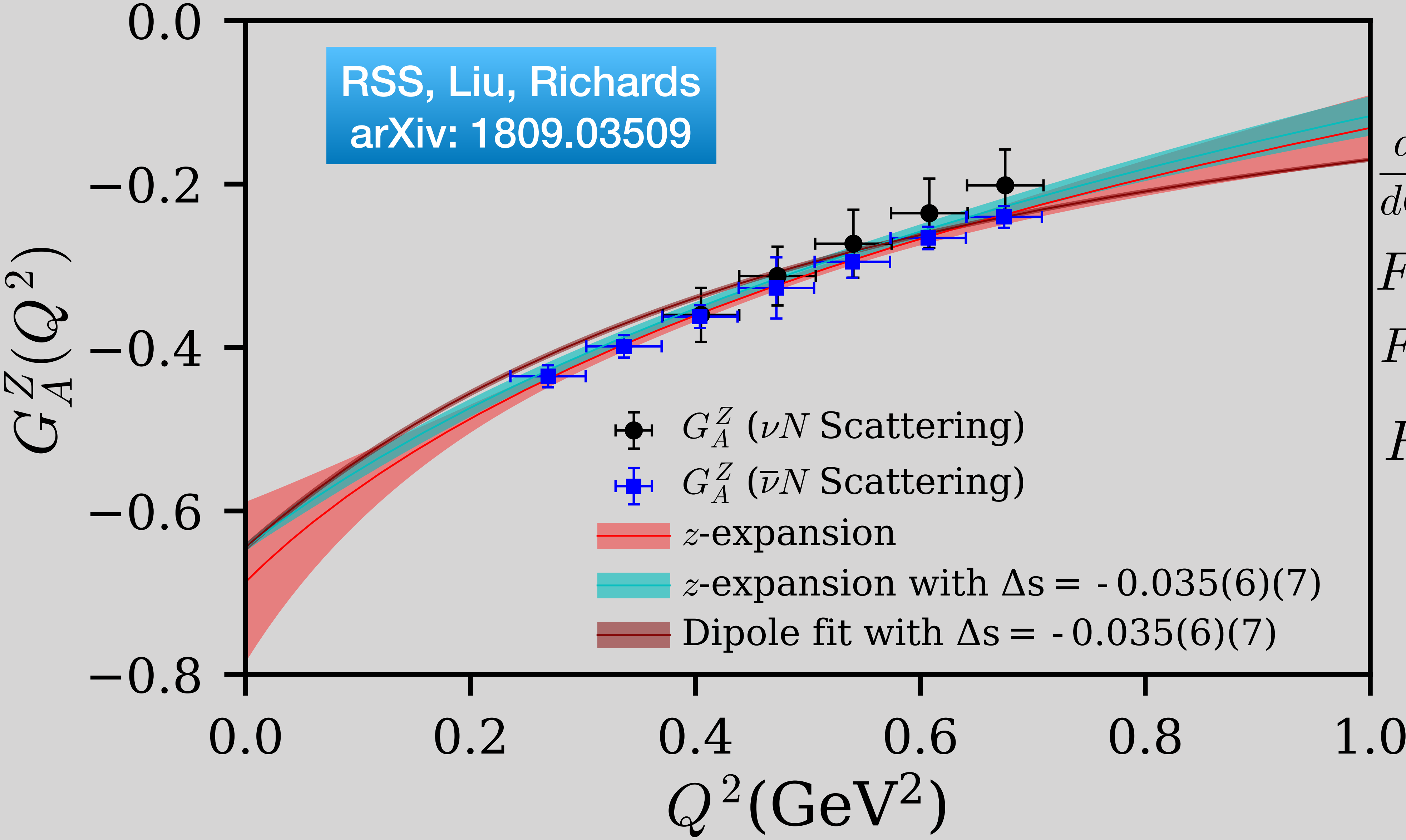

$\frac{d\sigma}{dQ^2}$ From MiniBooNE

$\left.\begin{matrix} F_{1,2}^p \\ F_{1,2}^n \end{matrix}\right\}$ From Experiment

$F_{1,2}^s$ From Lattice QCD

$$\boxed{G_A^s(0) = -0.035(6)(7)}$$

Lattice QCD
Liang, Yang, et. al. PRD 2018

$$\boxed{G_A^Z(0) = \frac{1}{2}\left(-G_A^{CC}(0) + G_A^s(0)\right) = -0.654(3)(5)}$$

No nuclear model dependence and experimental systematics on this value of $G^Z_A(0)$

Determination of Neutral Current Weak Axial FF

★ **Without Lattice input of strange quark axial charge**

$$G_A^Z(0) = -0.687(89)(40)$$

z-exp fit	Fit parameters	$G_A^Z(0)$
2-terms	$a_1 = 1.286(96)$	-0.726(30)
3-terms	$a_1 = 0.881(426), a_2 = 0.787(716)$	-0.678(65)
4-terms	$a_1 = 0.972(524), a_2 = 0.409(879),$ $a_3 = 0.537(1.542)$	-0.687(89)

★ **Dipole fit result with lattice QCD constraint of strange axial charge**

$$G_A^Z(Q^2) = \frac{G_A^Z(0)}{1 + \left(\frac{Q^2}{{M_A^{\mathrm{dip}}}^2}\right)^2}$$

$$M_A^{\mathrm{dip}} = 1.057(14)\ \mathrm{GeV}$$

For reference
Not used in analysis

★ Possibility: Since strange quark contribution is small set

$$G^s_{E,M} = 0 \quad \text{(??)}$$

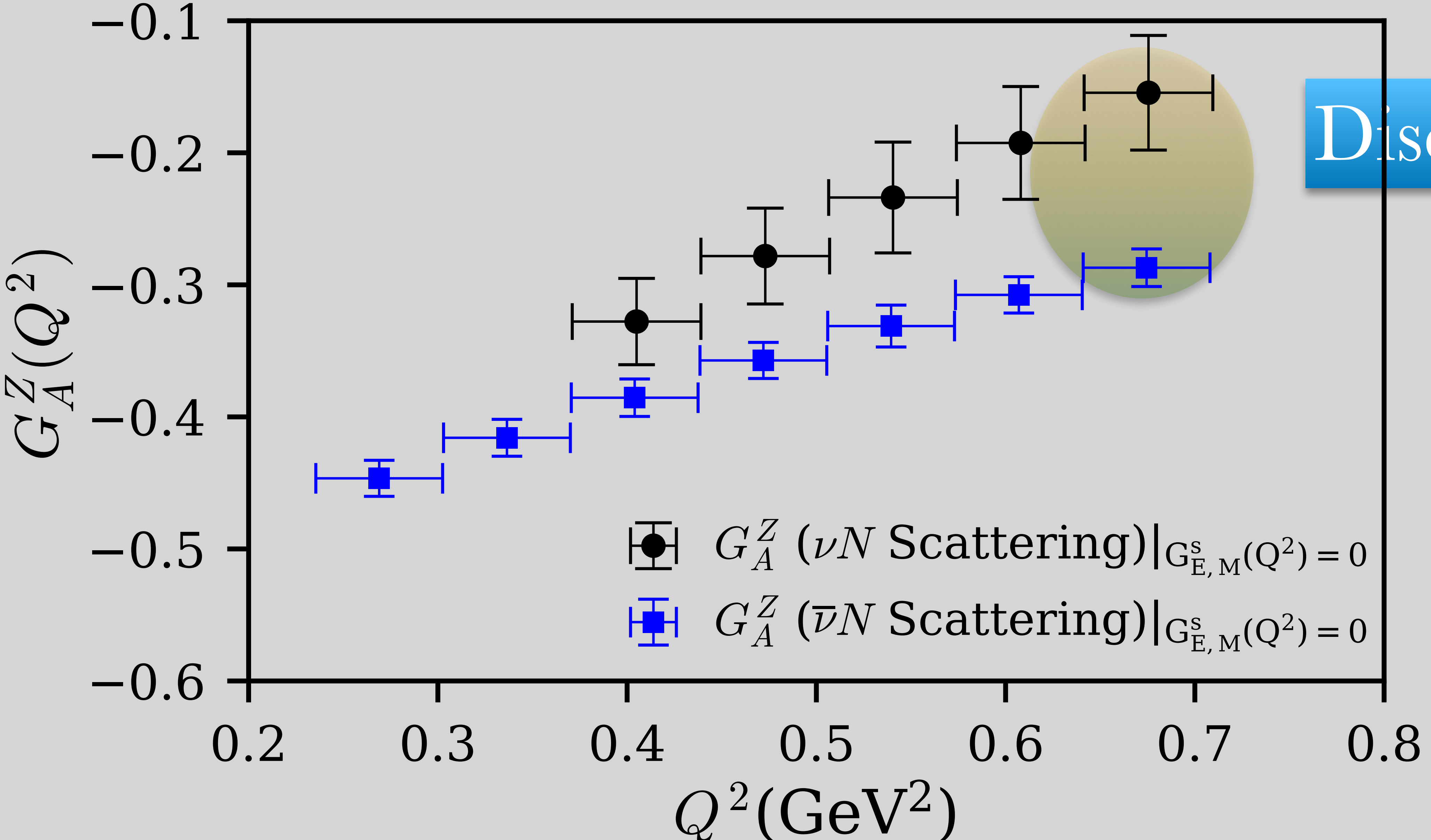

Discrepancy !!

$$\cancel{G^s_{E,M} = 0}$$

Reconstruction of MiniBooNE Differential Cross Sections

Lattice QCD calculation of strange quark axial charge is very important for low momentum transfer region

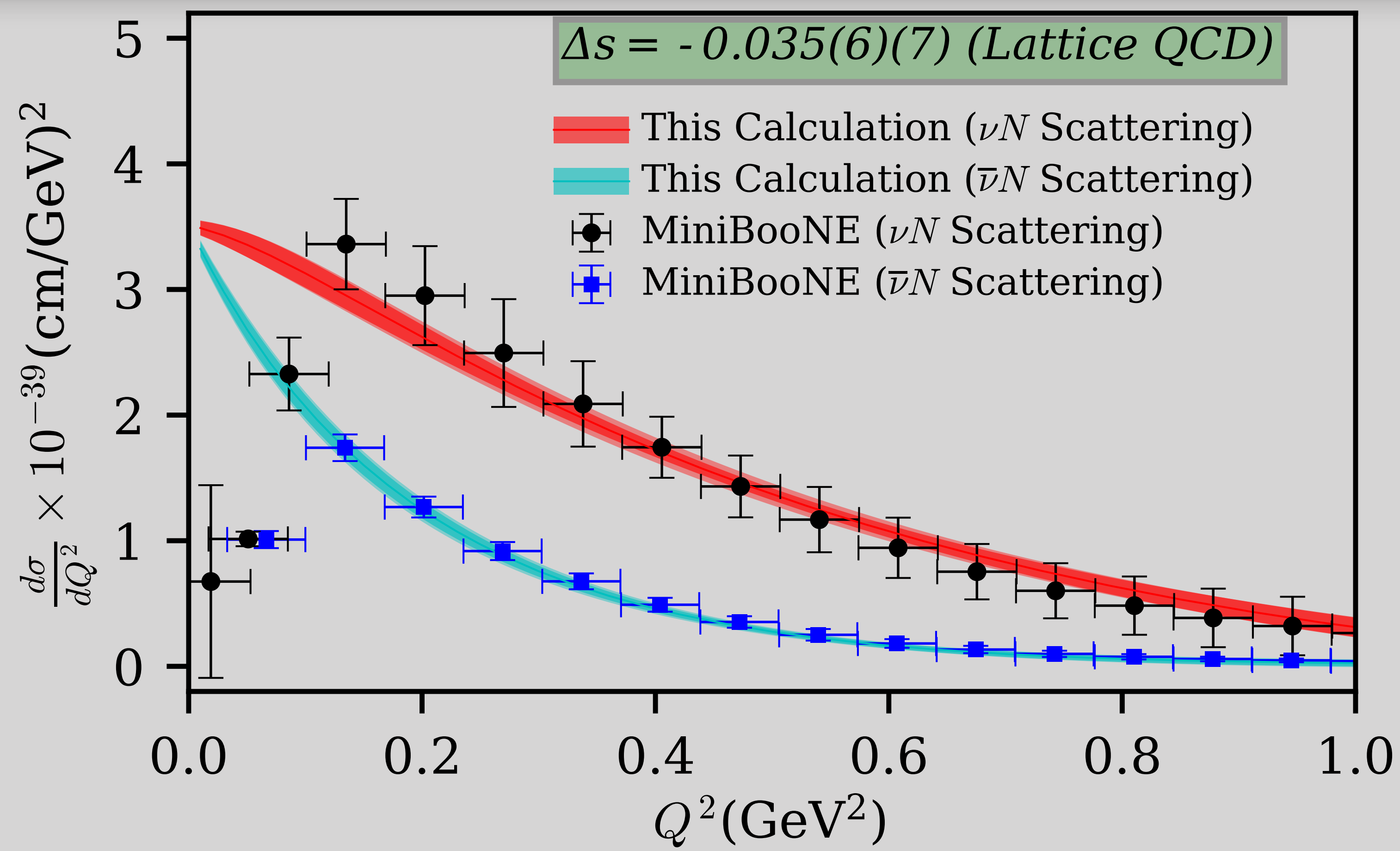

Unambiguous estimate of nuclear effects momentum transfer ~ 0

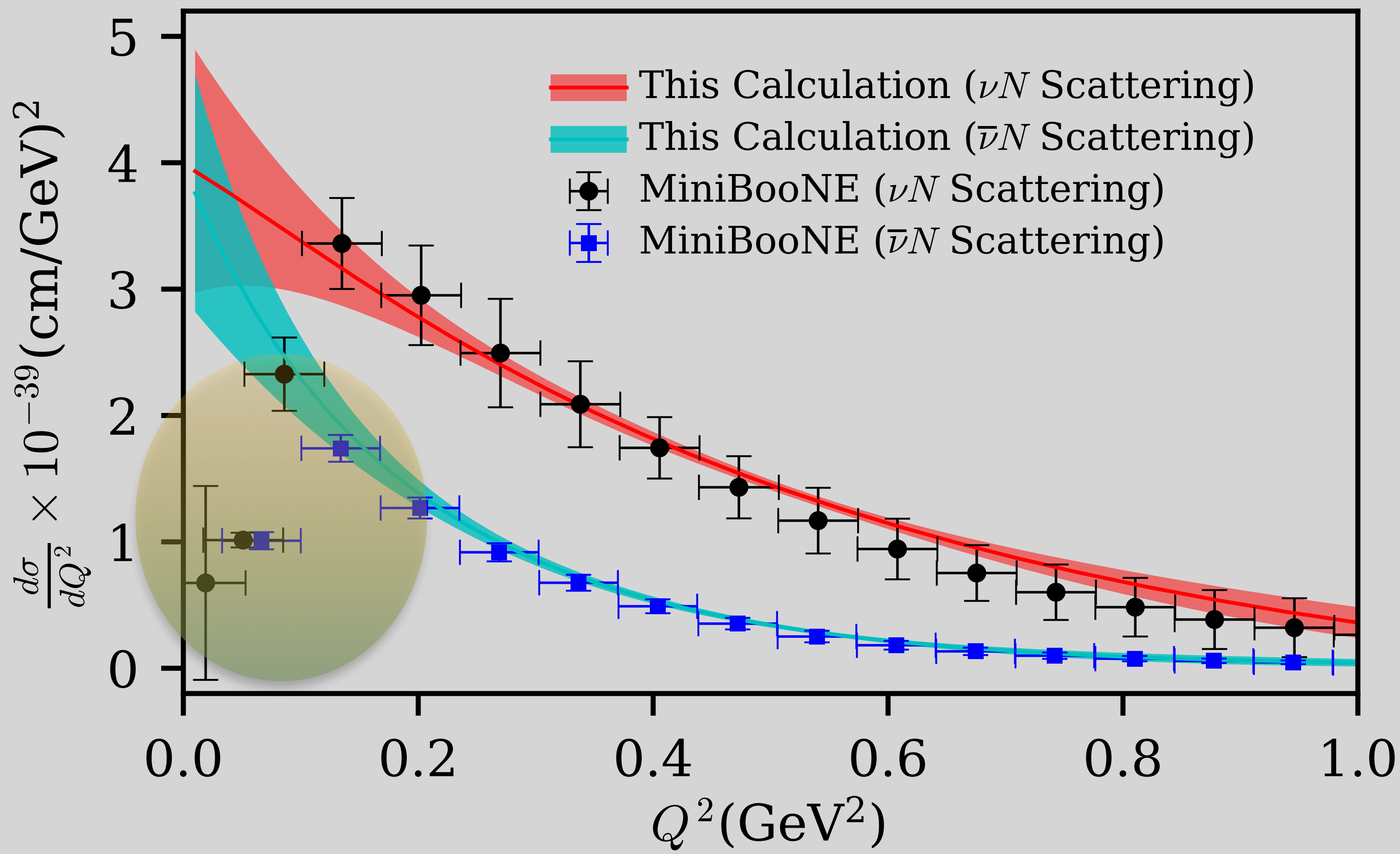

Prediction of BNL E734 Experimental Differential Cross Sections

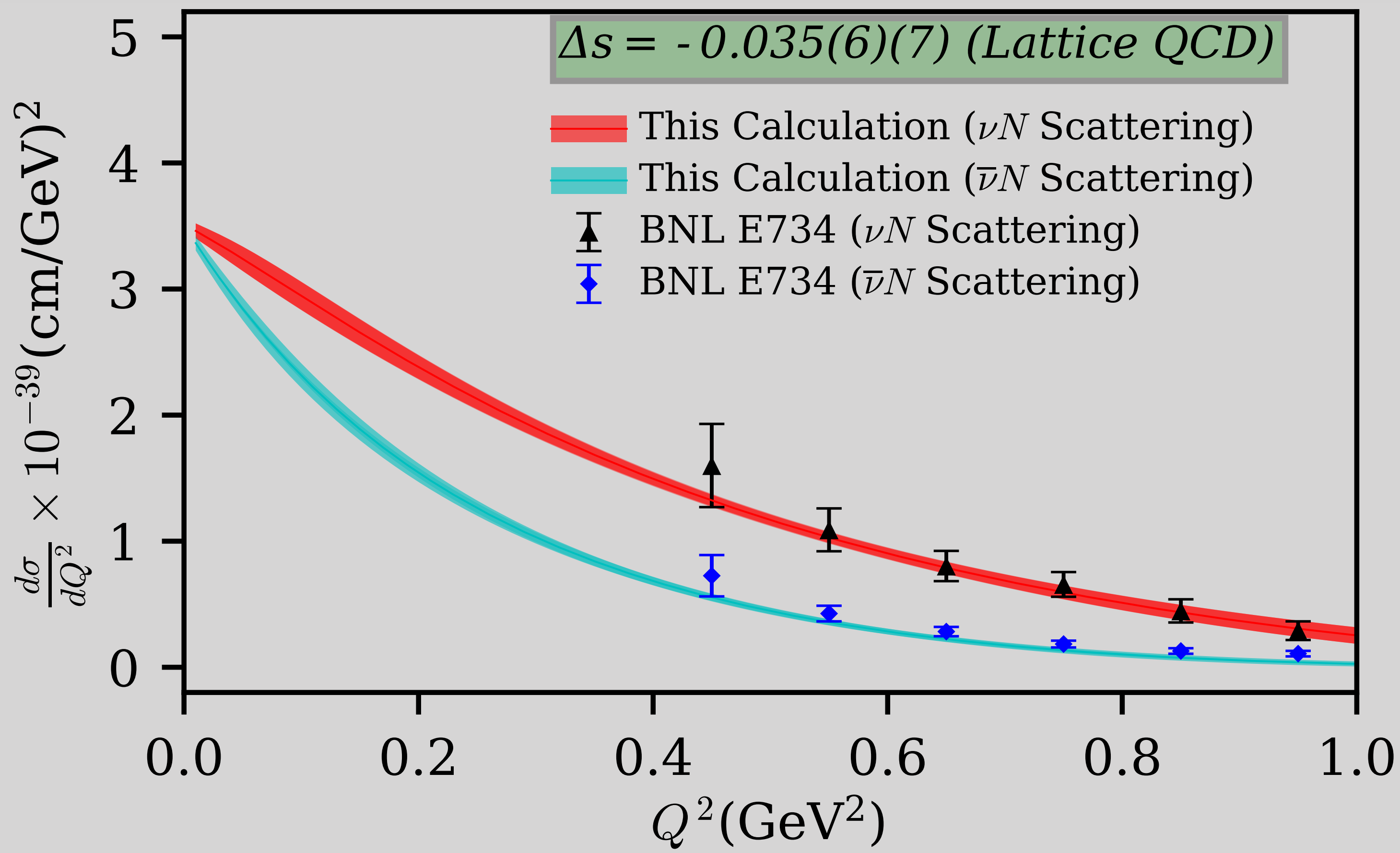

BNL E734 data was not used in the analysis

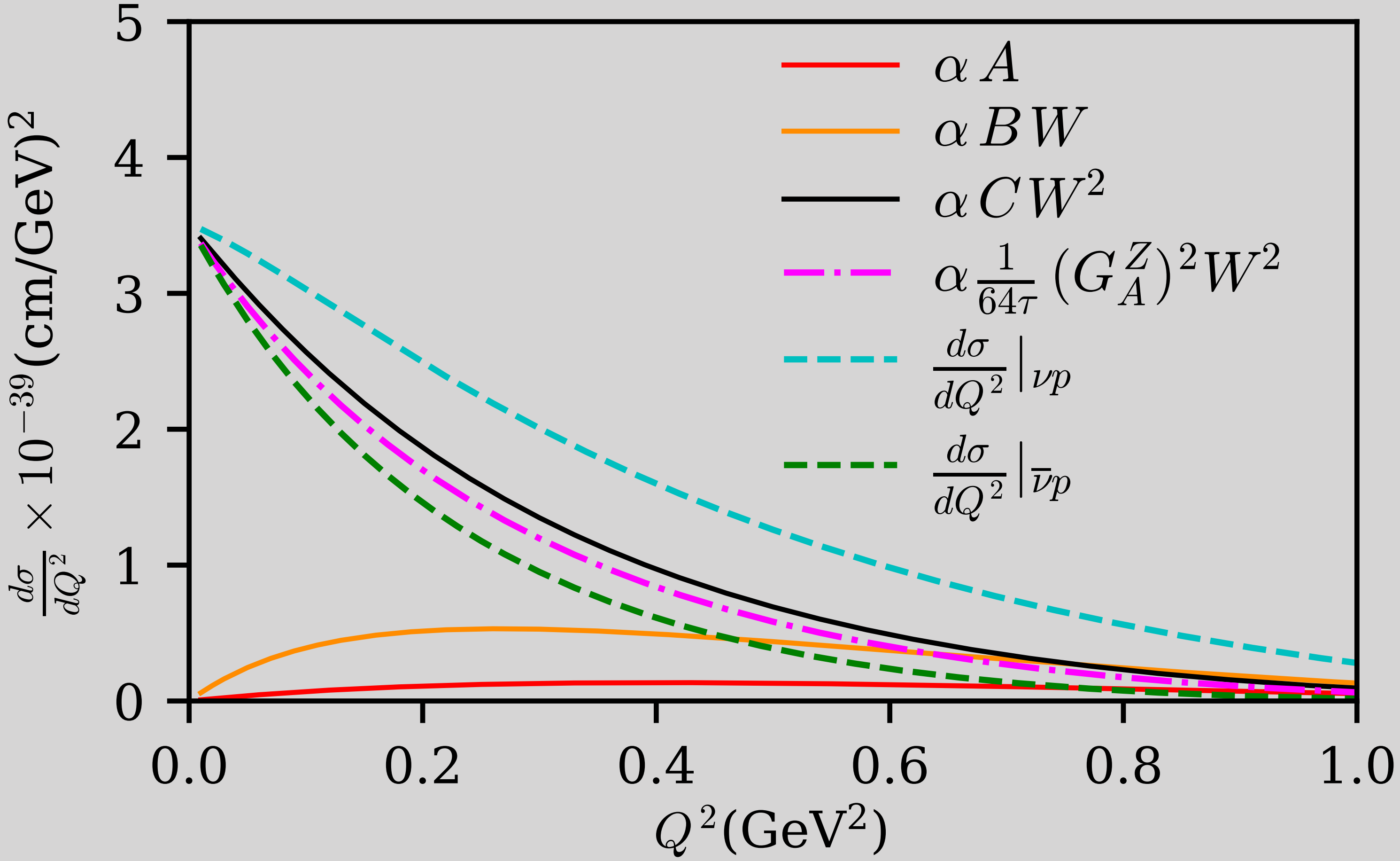

Neutral weak axial FF contributes the most

Charm Electric Form Factor
(First Calculation - To Appear Soon)

Preliminary

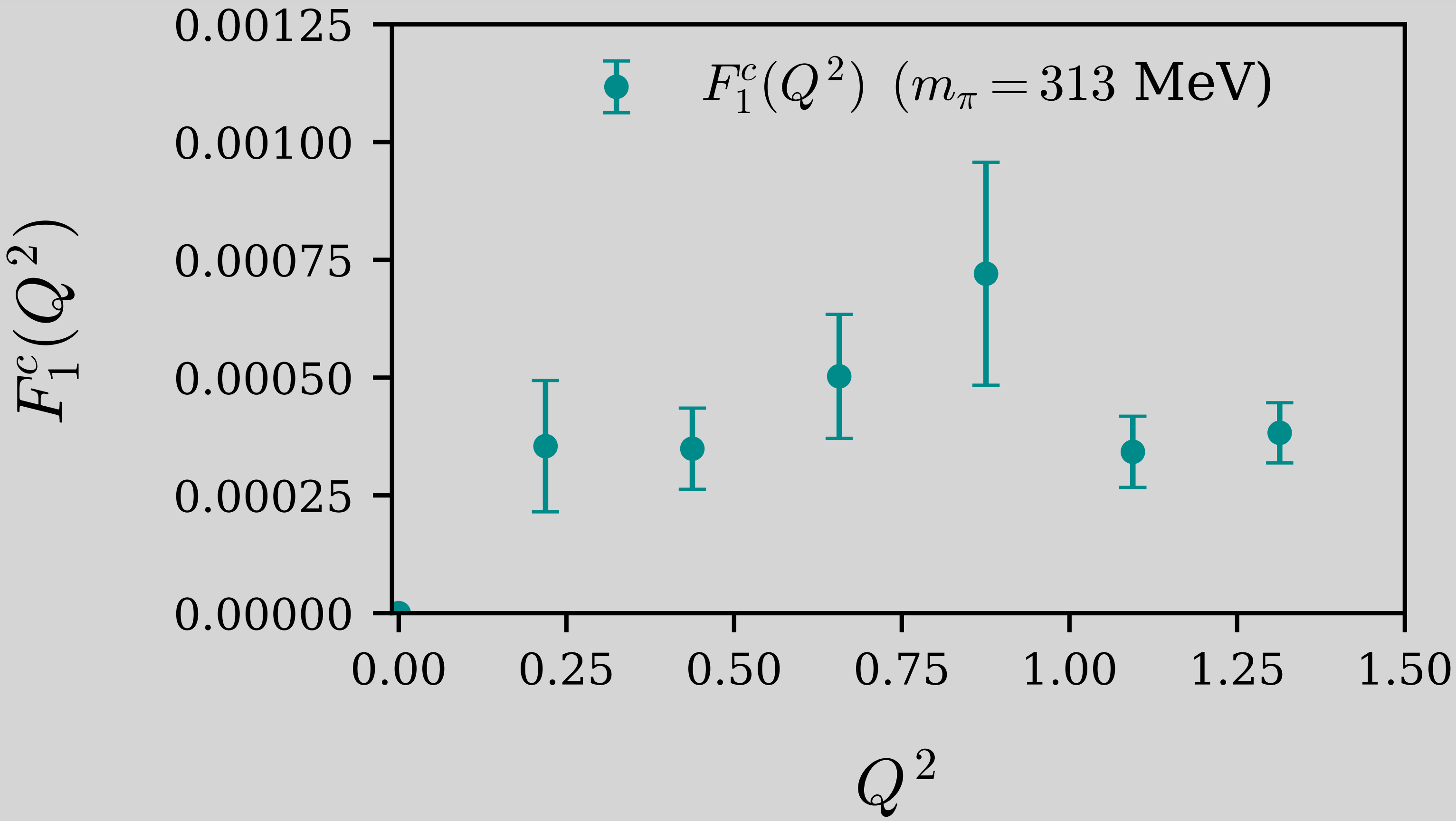

$$L^3 \times T = 32^3 \times 64$$

$$a = 0.083 \;\; \text{fm}$$

Notice the lowest and largest momentum transfer accessible on these Lattices

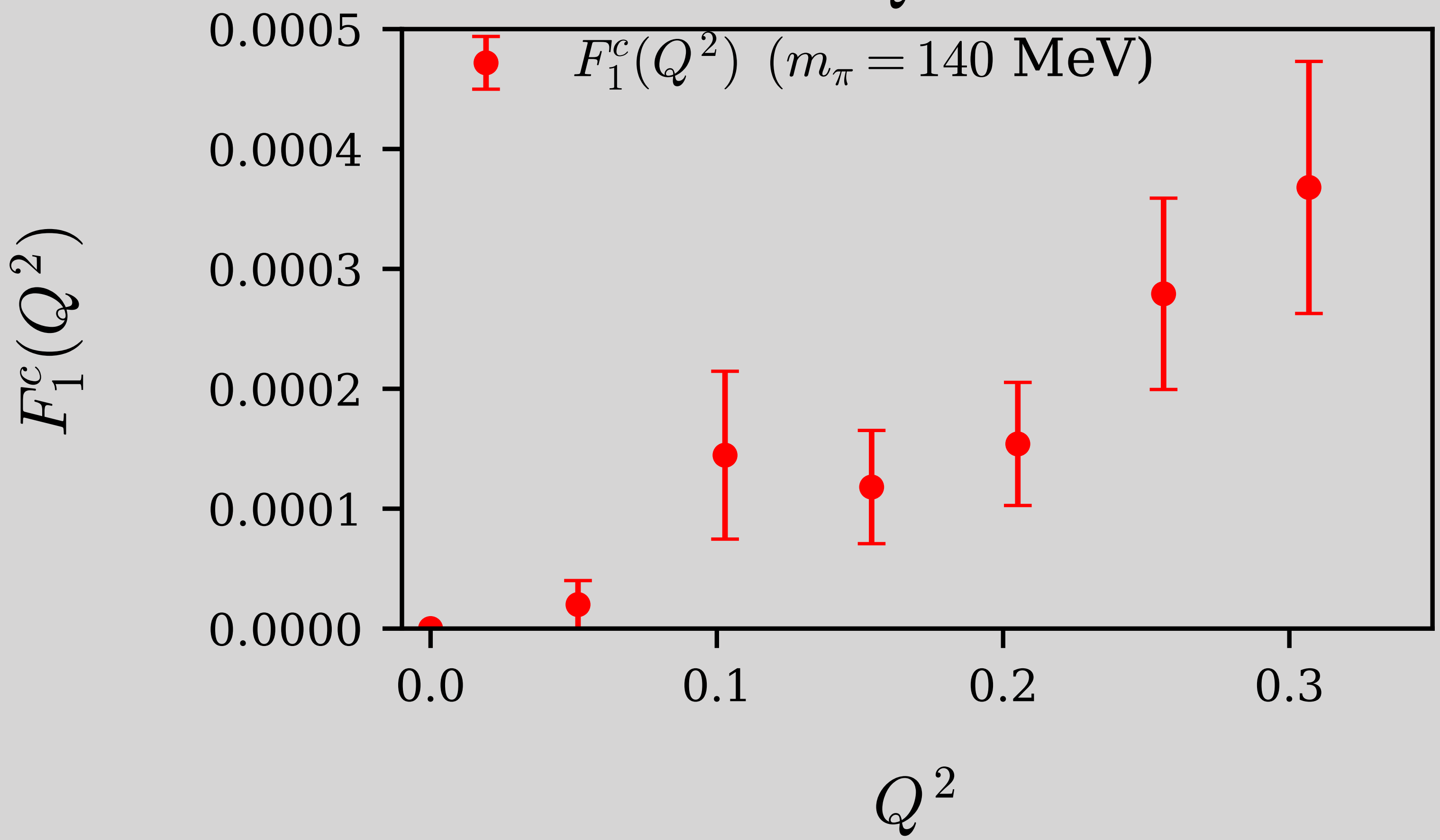

$$L^3 \times T = 48^3 \times 96$$

$$a = 0.11 \;\; \text{fm}$$

More Applications: Strange Electric FF

★ Strange-quark sea in nucleon has extrinsic $(g \to s\bar{s})$ and intrinsic components

★ Equal no. of s and $\bar{s}$ required by their non-valence nature in nucleon

$$\boxed{\langle s - \bar{s} \rangle = \int_0^1 dx [s(x) - \bar{s}(x)] = 0}$$

★ Nothing prohibits different $s(x)$ and $\bar{s}(x)$ distribution

★ Assuming strange-antistrange asymmetry is the only source to solve NuTeV anomaly ($\sin^2 \theta_W = 0.2276$)

$$\langle S_- \rangle \equiv \langle x(s - \bar{s}) \rangle = \int_0^1 dx\, x[s(x) - \bar{s}(x)] = 0.005 \quad \text{required}$$

More Applications: Strange Electric FF

★ Nonzero strange electric form factor

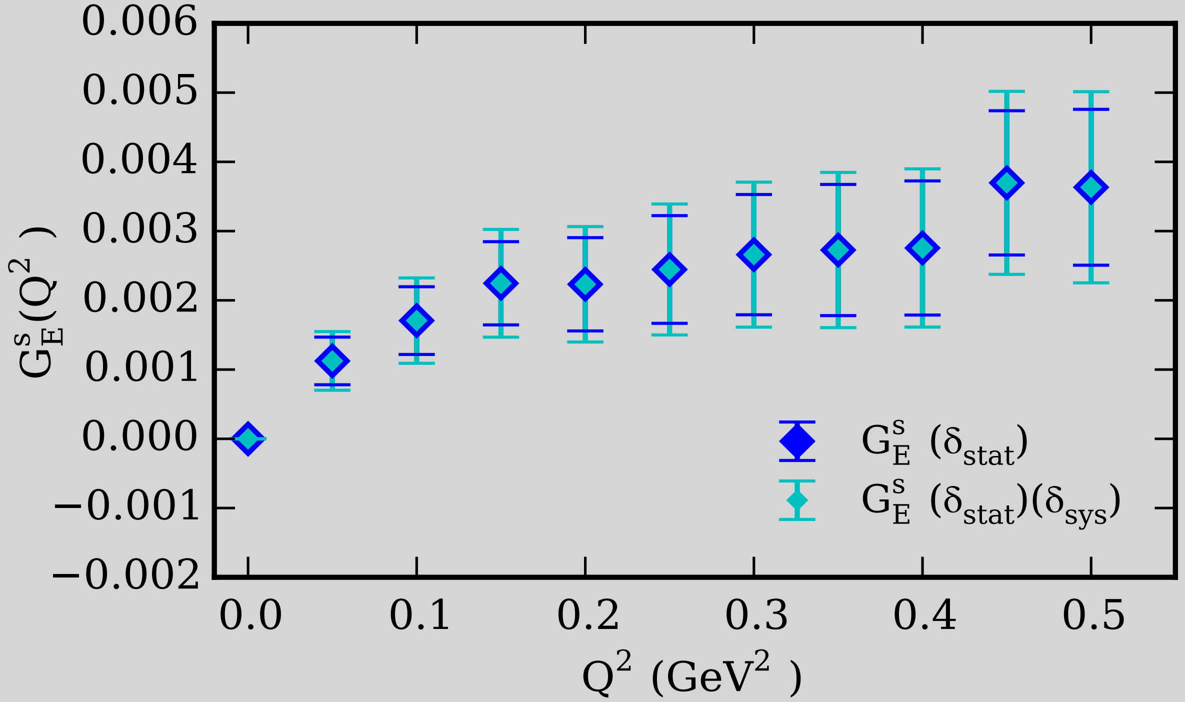

Signal, Thomas
PLB 191, 205 (1987)

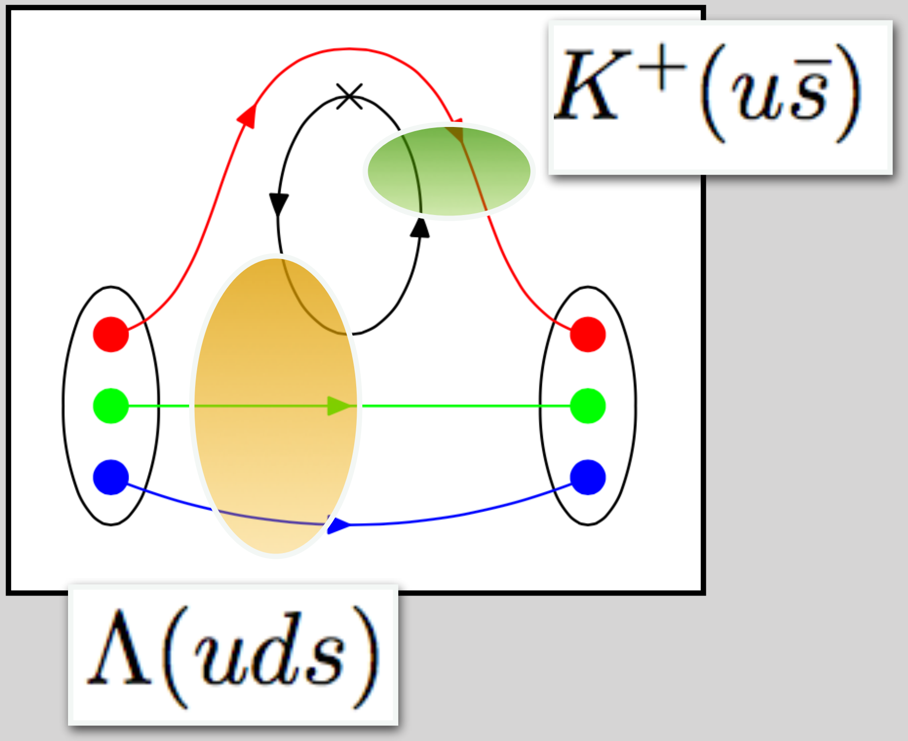

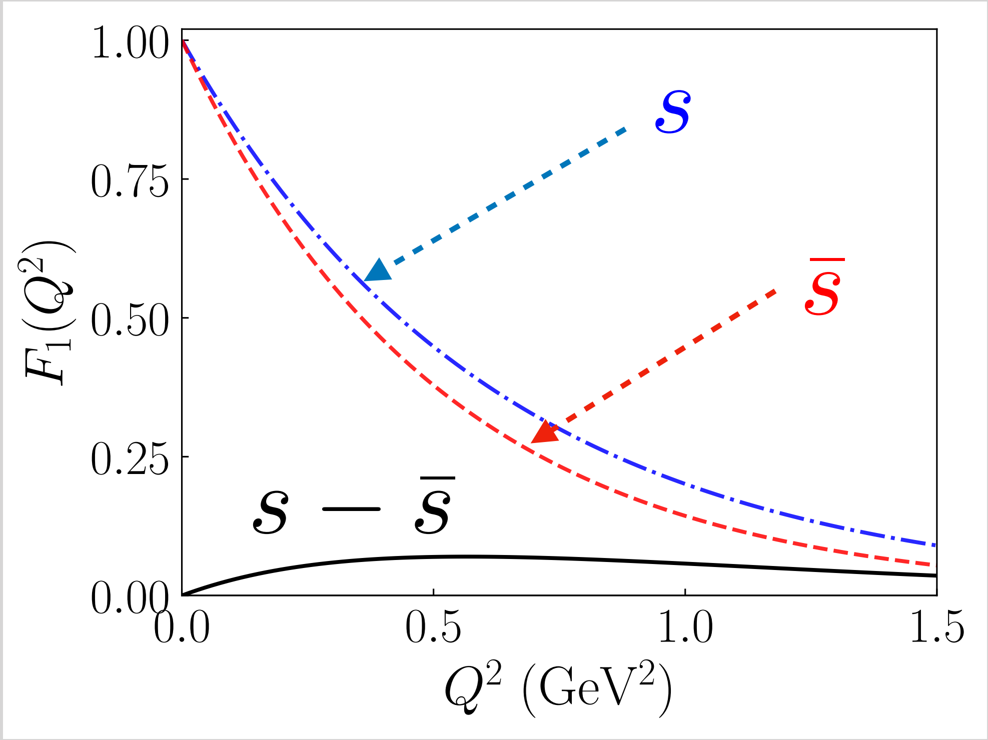

Fourier transform:
a narrower distribution in coordinate space corresponds to a wider distribution in momentum space

Constraints on strange-antistrange asymmetry

★ No definitive results from global fits

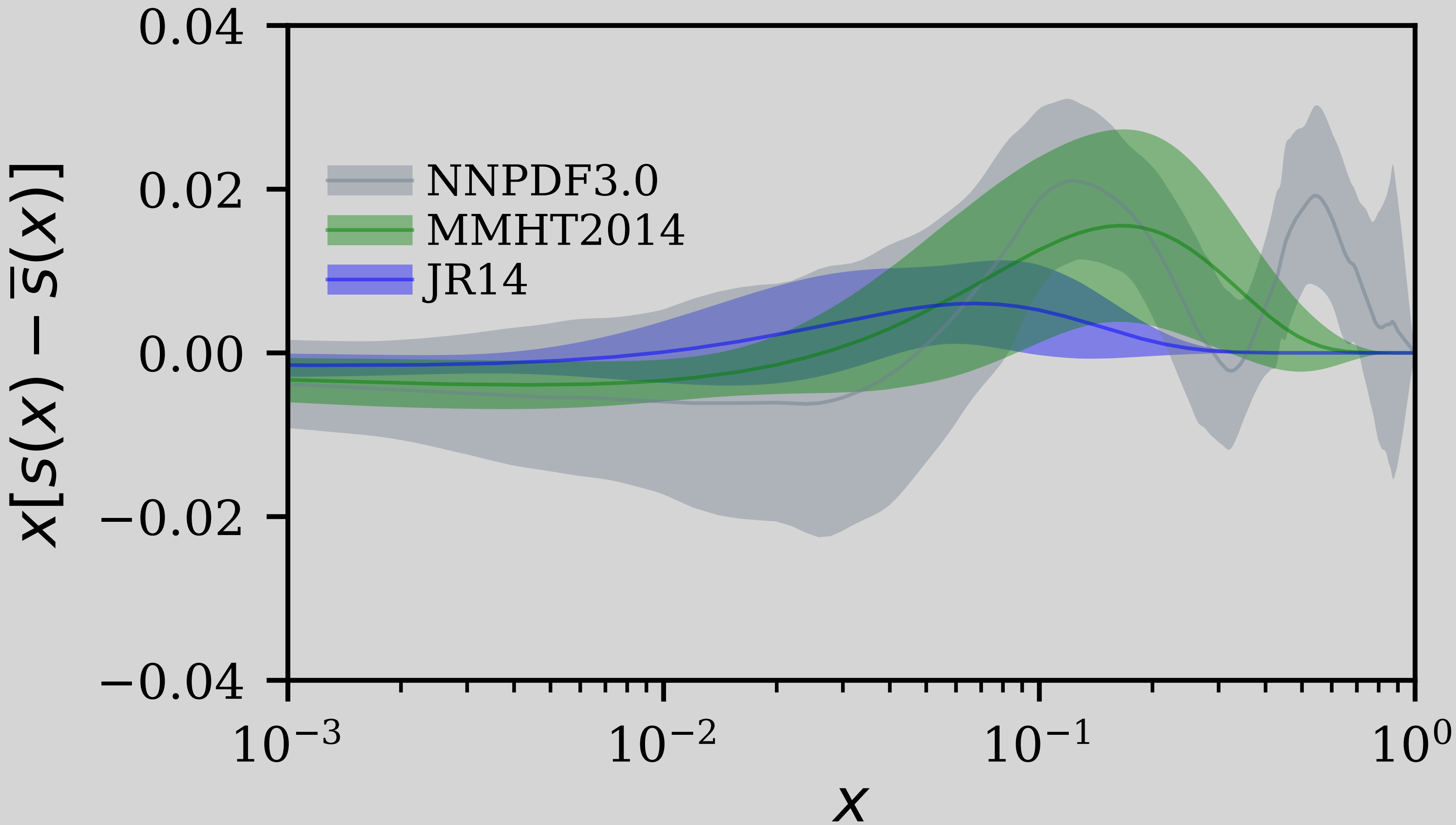

★ Nonzero strange electric form factor can be connected to strange-antistrange asymmetry in the nucleon's wave function

★ One Goal: Constrain unknown normalization of model calculations using Lattice QCD

Constraints on strange-antistrange asymmetry

★ Light-front holographic QCD : A semiclassical approach to relativistic bound state equations followed from the holographic embedding of light-front dynamics in a higher dimensional gravity theory

★ EM form factors for a bound state hadron of twist τ

$$F_\tau(t) = \frac{1}{N_\tau} B\big(\tau - 1, 1 - \alpha(t)\big)$$

$$N_\tau = \Gamma(\tau - 1)\Gamma(1 - \alpha(0))/\Gamma(\tau - \alpha(0))$$

$$\alpha(t) = \frac{1}{2} + \frac{t}{4\lambda} - \frac{\Delta M^2}{4\lambda}$$

de Téramond, Liu, RSS, Dosch, Brodsky, Deur PRL 2018

★ Write beta function in a reparametrization invariant form

$$B(u, v) = \int_0^1 dx\, w'(x)\, w(x)^{u-1} \left(1 - w(x)\right)^{v-1}$$

$$w(0) = 0, \quad w(1) = 1, \quad w'(x) \geq 0$$

$$w(x) = x^{1-x} e^{-a(1-x)^2}$$

Constraints on strange-antistrange asymmetry

★ Re-write form factor

$$F_\tau(t) = \frac{1}{N_\tau}\int_0^1 dx\, w'(x) w(x)^{-\frac{t}{4\lambda}-\frac{1}{2}}\left[1-w(x)\right]^{\tau-2} e^{-\frac{\Delta M^2}{4\lambda}\log\left(\frac{1}{w(x)}\right)}$$

★ Quark distribution

$$q_\tau(x) = \frac{1}{N_\tau}[1-w(x)]^{\tau-2} w(x)^{-\frac{1}{2}} w'(x) e^{-\frac{\Delta M^2}{4\lambda}\log\left(\frac{1}{w(x)}\right)}$$

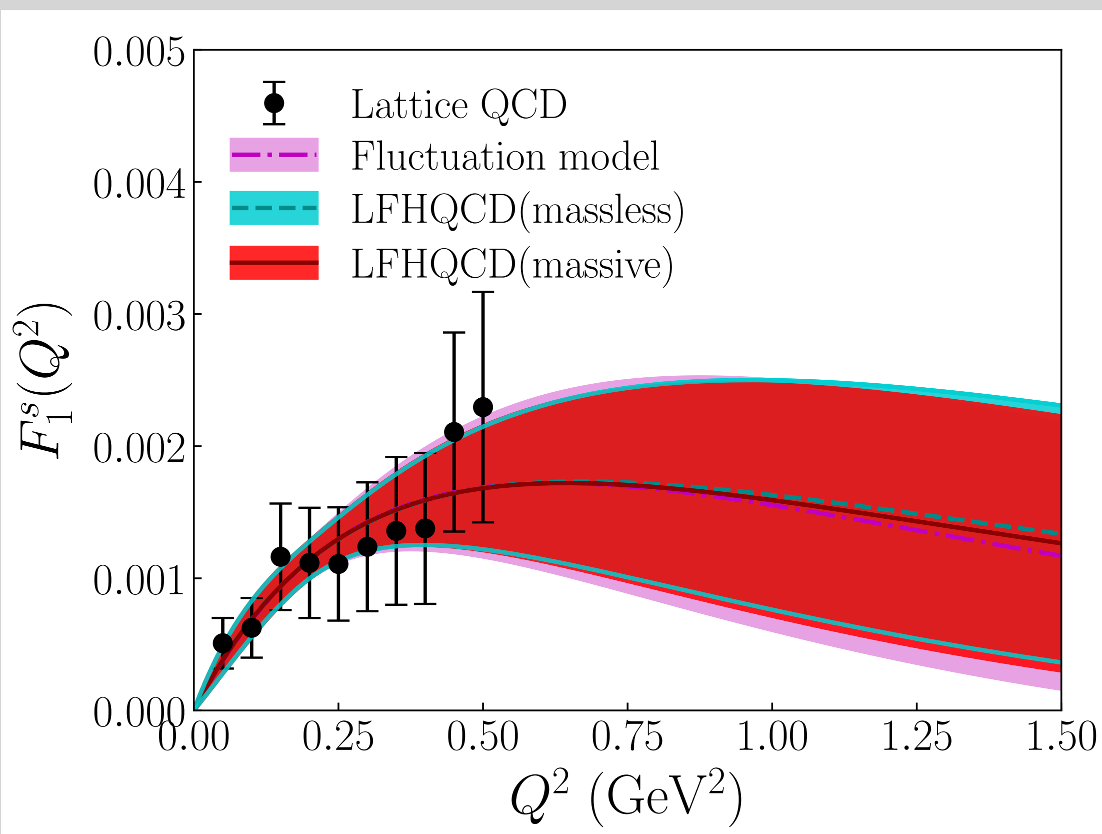

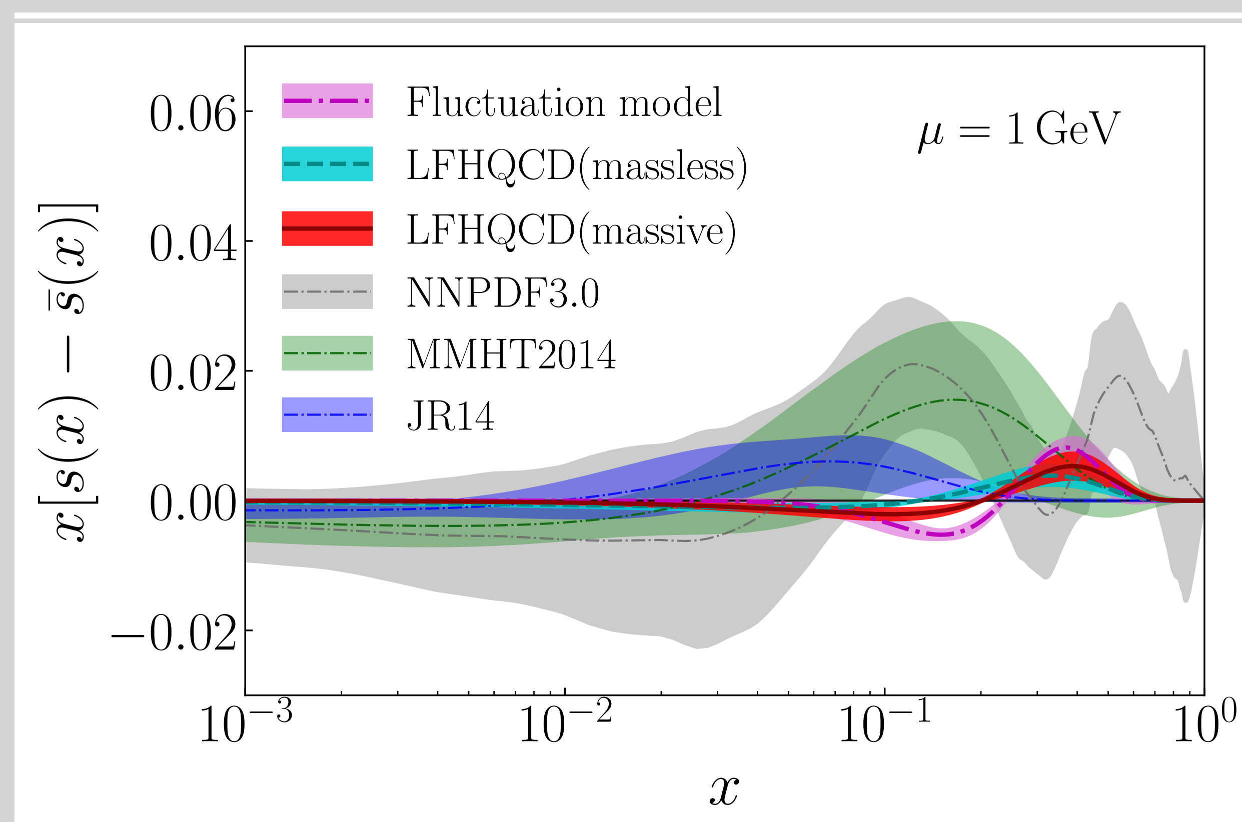

RSS, Liu, de Téramond, Dosch, Brodsky, et. al.
PRD 2018

$$\boxed{\langle S_- \rangle = 0.0011(4)}$$

Summary

- ★ A complete first-principles calculation of neutrino-nucleon scattering cross section is in progress

- ★ Lattice QCD inputs for neutrino-nucleon scattering can help experimentalists and many-body nuclear theorists to understand nuclear effects better, especially in low momentum transfer region

- ★ The interplay of first-principles lattice QCD calculations and experimental results can unveil nucleon properties to higher precision and accuracy than either theory or experiment alone can attain

- ★ Precise values of various matrix elements obtained from lattice QCD calculation can constrain different model calculations and can provide better understanding of the experimental data

Thank you

EXTRA

Overlap Fermion

Lattice version of of GW relation

$$D\gamma_5 + \gamma_5 D = D\gamma_5 D$$

A solution of this equation has been found in the form of an overlap operator

$$D_{ov} = 1 + \gamma_5 \operatorname{sign}(H), \quad H = \gamma_5 D$$

where D is some suitable kernel Dirac operator that is γ_5-hermitian, $\gamma_5 D\gamma_5 = D^\dagger$. Since H is hermitian, the matrix sign function is well-defined through the spectral theorem, therefore the overlap fermion is also γ_5-hermitian. Then

$$\begin{aligned} D_{ov}D_{ov}^\dagger &= (1 + \gamma_5 \operatorname{sign}(H))(1 + \operatorname{sign}(H)\gamma_5) \\ &= 1 + \gamma_5 \operatorname{sign}(H) + \operatorname{sign}(H)\gamma_5 + 1 + \gamma_5 \operatorname{sign}(H) \operatorname{sign}(H)\gamma_5 \\ &= 1 + \gamma_5 \operatorname{sign}(H) + \operatorname{sign}(H)\gamma_5 + 1 \\ &= D_{ov} + D_{ov}^\dagger. \end{aligned}$$

$$\begin{aligned} D(m,\rho) &= \rho D_{ov}(\rho) + m\left(1 - \frac{D_{ov}(\rho)}{2}\right) \\ &= \rho + \frac{m}{2} + \left(\rho - \frac{m}{2}\right)\gamma_5 \operatorname{sign}(H) \end{aligned}$$

$$\partial_\mu A^0_\mu = \sum_{f=u,d,s} 2m_f P_f - 2iN_f q$$

$$P_f = \bar{\psi}_f i\gamma_5 \psi_f, \qquad q = \frac{1}{16\pi^2} G^a_{\mu\nu} \tilde{G}^a_{\mu\nu}$$

$$A^0_\mu = \bar{\psi}_u i\gamma_\mu \gamma_5 \psi_u + \bar{\psi}_d i\gamma_\mu \gamma_5 \psi_d + \bar{\psi}_s i\gamma_\mu \gamma_5 \psi_s$$

$$\partial_\mu A^0_\mu \left(1 + \gamma N_f \frac{1}{\epsilon}\right) = \sum_{f=u,d,s} 2m^R_f P^R_f + \left(-2iN_f q + \gamma N_f \frac{1}{\epsilon} \partial_\mu A^0_\mu\right)$$

$$\gamma = -(\alpha_s/\pi)^2 \tfrac{3}{8} C_F.$$

$$< p|A^{\dagger\mu}|n > \;=\; \bar{p}\left[\gamma_\mu F_A \gamma_5 + \frac{q_\mu}{M} F_P \gamma_5\right] n.$$

(a) pion vertex correction

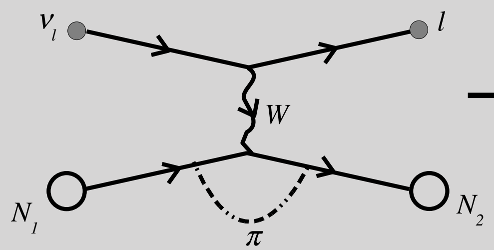

Axial Part

$$A \;\sim\; [n \to p + \pi] \times [\pi - propagator] \times [\pi \to l + \nu],$$

$$A \;\sim\; [ig_0(\bar{p}\gamma_5 n)] \times \left[\frac{1}{q^2 - m_\pi^2}\right] \times \left[\frac{G_F cos\theta_c}{\sqrt{2}} i f_\pi q_\mu (\bar{l}\gamma^\mu(1-\gamma_5)\nu)\right]$$

pion-nucleon coupling

(b) pion One-pion exchange

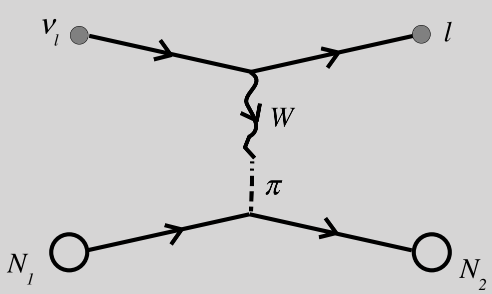

$$< p|A^{\dagger\mu}|n > \;=\; \bar{p}\left[\gamma_\mu F_A - \frac{q_\mu}{M}\frac{g_0 f_\pi}{q^2 - m_\pi^2}\right]\gamma_5 n$$

Although the axial current is not conserved, it may be approximately conserved in $m_\pi \to 0$ limit (partial conservation of axial current), $\lim_{m_\pi \to 0} \partial_\mu A^\mu = 0$.

$$g_0 f_\pi \;=\; 2M^2 F_A$$

$$F_P \;=\; -\frac{g_0 f_\pi}{q^2 - m_\pi^2} = \frac{2M^2}{Q^2 + m_\pi^2} F_A$$

MiniBooNE cross section model

39% charged current quasi-elastic (CCQE), $\nu_\mu + p \to \mu^- + n$;

16% neutral current elastic (NCE), $\nu_\mu + p(n) \to \nu_\mu + p(n)$;

25% charged current one π^+ production (CC1π^+), $\nu_\mu + p(n) \to \mu^- + \pi^+ + p(n)$;

4% charged current one π° production (CC1π°), $\nu_\mu + n \to \mu^- + \pi^\circ + p$;

4% neutral current one $\pi^\pm$ production (NC1$\pi^\pm$), $\nu_\mu + p(n) \to \mu^\mp + \pi^\pm + n(p)$;

8% neutral current one π° production (NC1π°), $\nu_\mu + p(n) \to \mu^- + \pi^\circ + p(n)$;

4% others, multi pion production (multiπ), deep inelastic scattering (DIS), etc.

1) For low values of s we observe resonances, for instance in $N - \pi$ scattering the Δ and higher resonances. This means that there are poles in the variable s at the resonance masses. The amplitude $T(s,t)$ behaves near the resonance as

$$T(s,t) \sim \frac{A}{s - m_R^2}$$

For unstable resonances m_R has an imaginary part.

2) For high values of s we have Regge behaviour, that is in that limit the amplitude behaves like

$$T(s,t) \sim s^{\alpha(t)},$$

the function $\alpha(t)$ is called a Regge trajectory.

This gives a good description of high energy scattering, that is for large values of s and for negative values of t. For positive values of t, which can occur in annihilation, a resonance pole with total angular momentum J occurs at those values of t, where $\alpha(t)$ is a nonnegative integer J. It turned out that linear trajectories, that is

$$\alpha(t) = \alpha_0 + \alpha' \cdot t \tag{1.1}$$

give a good description of the data. α_0 is called the intercept and α' the slope of the trajectory. The concept of duality was developed as an attempt to unify these two seemingly very different features.

An important model for scattering amplitudes which shows this dual behaviour is the **Veneziano model** $V(s,t)$ [8]. It consists of a sum of expressions like

$$T(s,t) = \frac{\Gamma(1-\alpha(s))\Gamma(1-\alpha(t))}{\Gamma(2-\alpha(s)-\alpha(t))} = \frac{\Gamma(1-\alpha_0-\alpha' s))\Gamma(1-\alpha_0-\alpha' t)}{\Gamma(2-\alpha_0-\alpha' s-\alpha_0-\alpha' t)} \tag{1.2}$$

$$T(s,t) = \frac{\Gamma(1-\alpha(s))\Gamma(1-\alpha(t))}{\Gamma(2-\alpha(s)-\alpha(t))} = \frac{\Gamma(1-\alpha_0-\alpha' s))\Gamma(1-\alpha_0-\alpha' t)}{\Gamma(2-\alpha_0-\alpha' s-\alpha_0-\alpha' t)} \tag{1.2}$$

with the linear trajectory $\alpha(x) = \alpha_0 + \alpha' x$. $\Gamma(z)$ is the Euler Gamma function which for integer values is the factorial, $\Gamma(z+1) = z!$. From the properties of the Γ function follows: for large values of s and negative values of t the amplitude $T(s,t)$ shows Regge behaviour, and it has resonance poles for for integer values of $\alpha(s)$ or $\alpha(t)$. These poles lie on straight lines, the lowest one is called the Regge trajectory, the ones above it are called daughter trajectories, see Fig. 1.2.

It was soon realized, that the Veneziano model corresponds to a string theory, where the rotation of the string gives the resonances along the Regge trajectories and the vibrational modes yield the daughter trajectories, see figure 1.3.

In this approach the hadrons are not point-like objects nor composed of point-like objects (elementary quantum fields), but they are inherently extended objects: strings.

$$H\phi(\zeta) = \left(-\partial_\zeta^2 + \frac{4L^2-1}{4\zeta^2} + U(\zeta)\right)\phi(\zeta) = M^2\phi(\zeta)$$

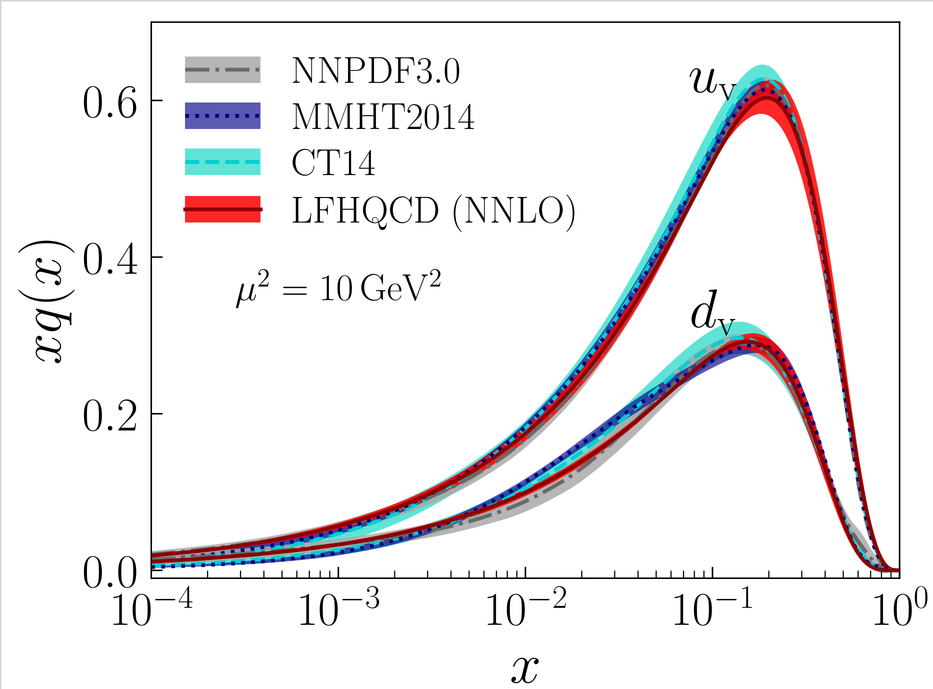
NNPDF3.0
MMHT2014
CT14
LFHQCD (NNLO)
u_v
d_v
$\mu^2 = 10\,\mathrm{GeV}^2$
$xq(x)$
x

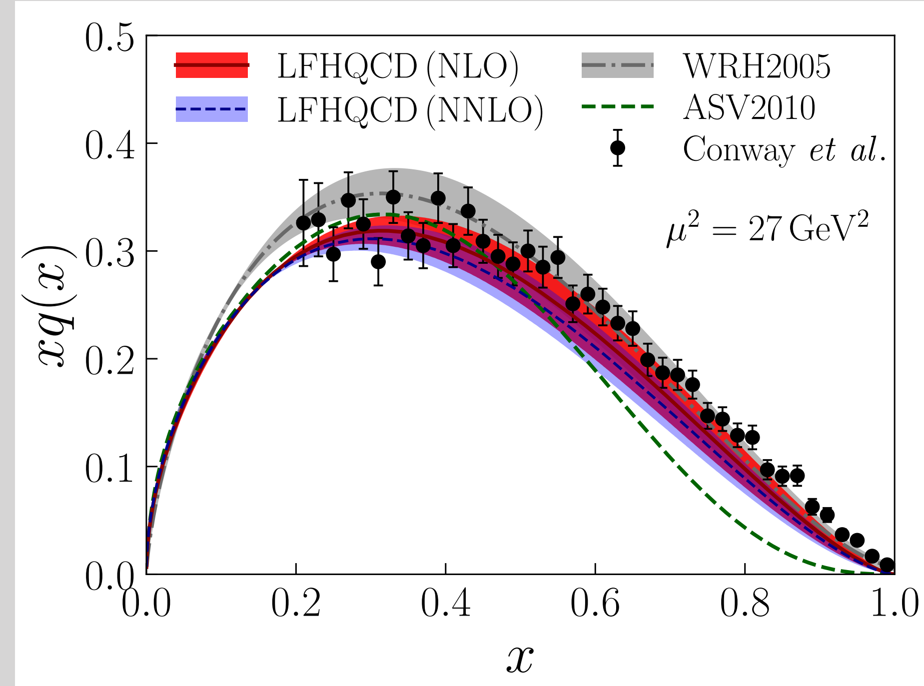
LFHQCD (NLO)
LFHQCD (NNLO)
WRH2005
ASV2010
Conway *et al.*
$\mu^2 = 27\,\mathrm{GeV}^2$
$xq(x)$
x

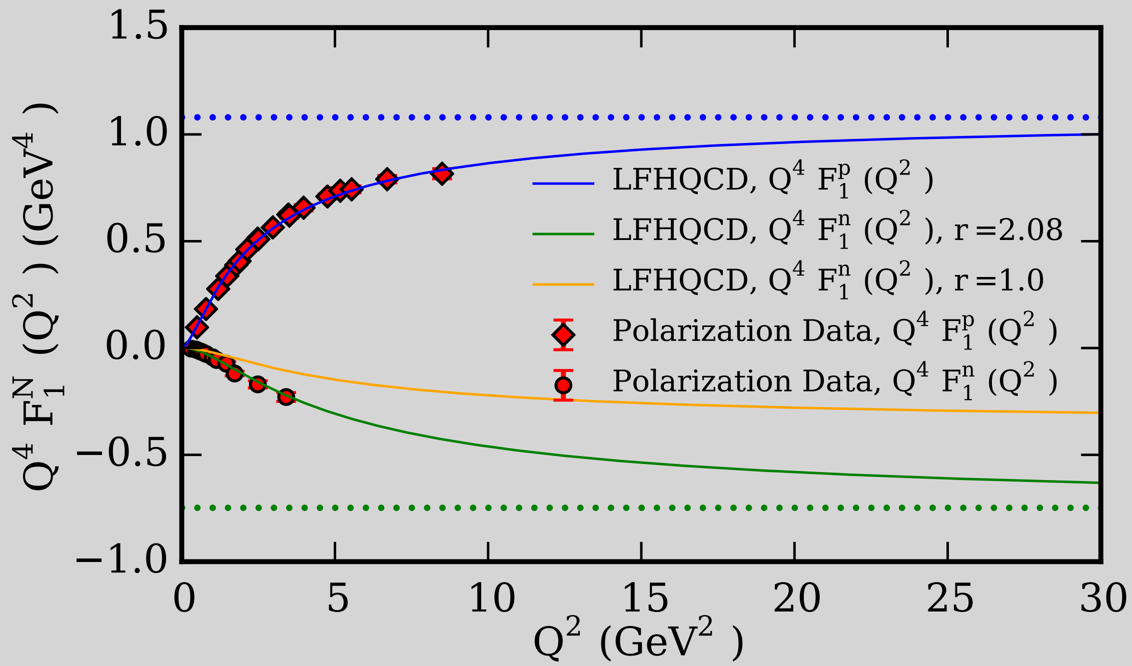
LFHQCD, $Q^4\ F_1^p\ (Q^2)$
LFHQCD, $Q^4\ F_1^n\ (Q^2)$, r =2.08
LFHQCD, $Q^4\ F_1^n\ (Q^2)$, r =1.0
Polarization Data, $Q^4\ F_1^p\ (Q^2)$
Polarization Data, $Q^4\ F_1^n\ (Q^2)$
$Q^4\ F_1^N\ (Q^2)\ (\mathrm{GeV}^4)$
$Q^2\ (\mathrm{GeV}^2)$

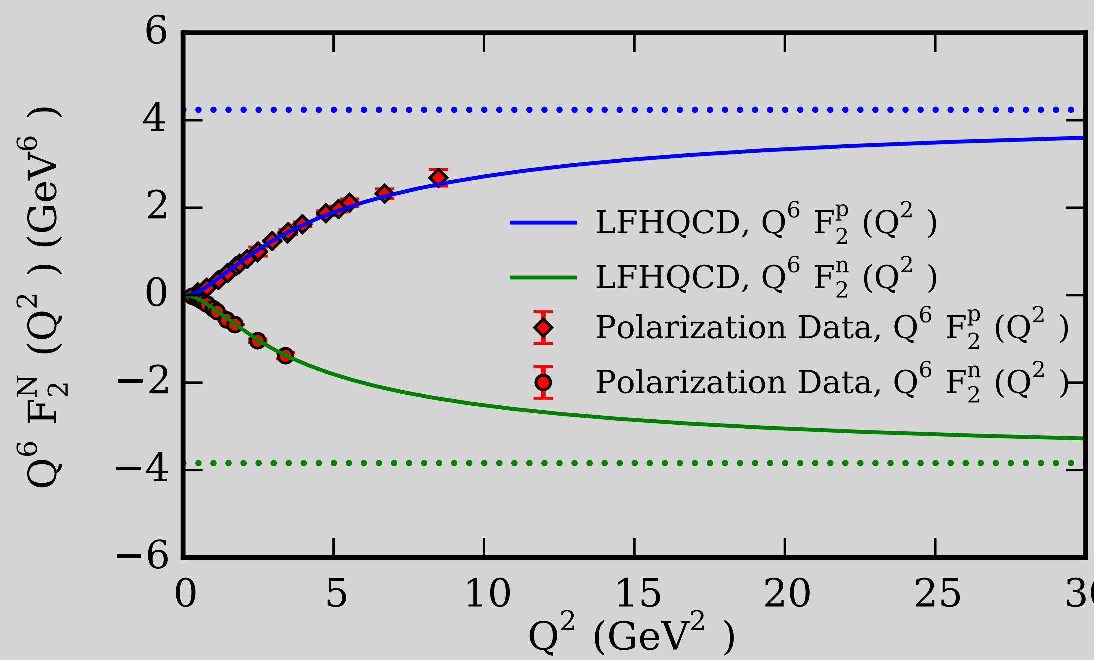
LFHQCD, $Q^6\ F_2^p\ (Q^2)$
LFHQCD, $Q^6\ F_2^n\ (Q^2)$
Polarization Data, $Q^6\ F_2^p\ (Q^2)$
Polarization Data, $Q^6\ F_2^n\ (Q^2)$
$Q^6\ F_2^N\ (Q^2)\ (\mathrm{GeV}^6)$
$Q^2\ (\mathrm{GeV}^2)$

$$P_{\nu_\alpha \to \nu_\beta}(t) = \sum_{k,j} U_{\alpha k}^* U_{\beta k} U_{\alpha j} U_{\beta j}^* \exp\left(-i \frac{\Delta m_{kj}^2 t}{2E}\right)$$

$$U_{\alpha k} = U_{\alpha k}^{\mathrm{D}} \, e^{i\lambda_k}$$

Neutrino oscillations are independent of Majorana phases which are always factorized in a diagonal matrix on the right of the mixing matrix CP and T violation in neutrino oscillation depends on the Dirac phases

$$\nu_\alpha \to \nu_\beta \xleftrightarrow{\mathrm{CP}} \bar{\nu}_\alpha \to \bar{\nu}_\beta$$

$$\nu_\alpha \to \nu_\beta \xleftrightarrow{\mathrm{T}} \nu_\beta \to \nu_\alpha$$

$$\nu_\alpha \to \nu_\beta \xleftrightarrow{\mathrm{CPT}} \bar{\nu}_\beta \to \bar{\nu}_\alpha$$

$$\mathcal{N}(A,Z) \to \mathcal{N}(A,Z+2) + 2\,e^- + 2\,\bar{\nu}_e \qquad (2\beta^-_{2\nu})$$

$$\mathcal{N}(A,Z) \to \mathcal{N}(A,Z-2) + 2\,e^+ + 2\,\nu_e \qquad (2\beta^+_{2\nu})$$

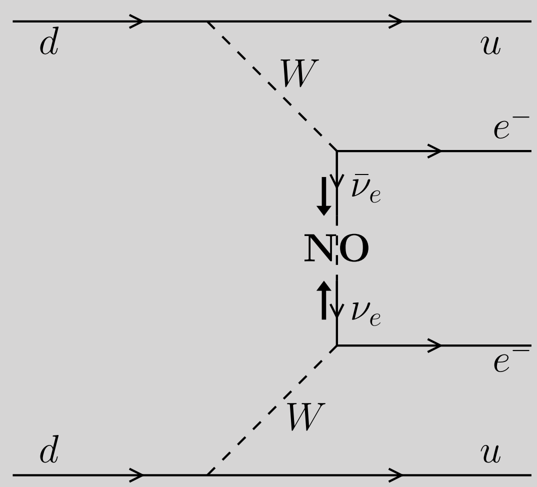

FIG. 14.8. Illustration of the two reasons why $2\beta^-_{0\nu}$ decay processes are forbidden in the SM: $\bar{\nu}_e \neq \nu_e$ and the helicity mismatch.

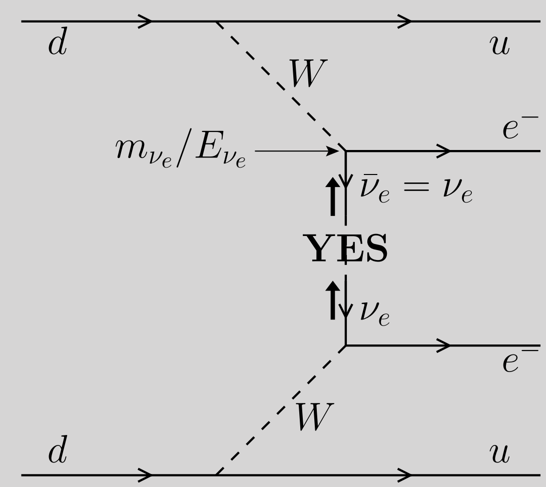

FIG. 14.9. Illustration of the particle–antiparticle and helicity matching conditions for $2\beta^-_{0\nu}$ decay.

The particle–antiparticle mismatch. A $\bar{\nu}_e$ emitted in the upper leptonic vertex cannot be absorbed in the lower leptonic vertex, which is capable only of absorbing a ν_e.

The helicity mismatch. The helicity of the neutral lepton emitted in the upper leptonic vertex is *positive* and the lower leptonic vertex can absorb only a neutral lepton with *negative* helicity.

Particle–antiparticle matching: $\bar{\nu}_e = \nu_e$. The electron neutrino must be a Majorana particle. In this case, the total lepton number is not conserved (see section 6.2.4).

Helicity matching: $m_{\nu_e} \neq 0$. In this case, the upper leptonic vertex can emit a neutrino with negative helicity with relative amplitude m_{ν_e}/E_{ν_e} (see eqn (6.106)), which is absorbed by the lower leptonic vertex with relative amplitude equal to unity.